8

Construction Loading in High-Rise Buildings

S.K. Ghosh, Ph.D., P.E.*

8.1 Introduction

Structural formwork and its support system must be given careful consideration in two different respects: (1) loads that are applied to the formwork and its supports, and (2) loads that the formwork and its supports apply to the structure. The first is the subject of Chapter 7 on formwork and falsework; the second is the subject of this chapter.

8.2 Construction Loads

8.2.1 Design Considerations

In the construction of multistory buildings with reinforced concrete floor slabs, a step-by-step sequence of operations is employed. The sequence is comprised of the steps of setting up shoring on the most recently poured floor, forming the next floor, setting up reinforcement, and concreting the slab. Because the floor below the one being concreted is usually only a few days old, it is common practice to leave

* President, S.K. Ghosh Associates, Inc., Palatine, Illinois, and Fellow of the American Concrete Institute; specializes in structural design, including wind- and earthquake-resistant design.

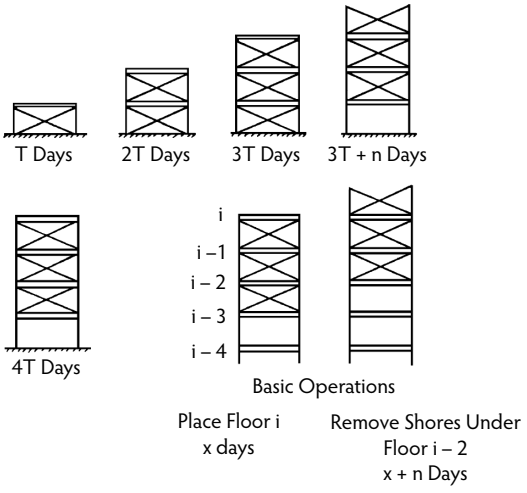

FIGURE 8.1 Construction sequence using three levels of shores.

formwork supports in place between that floor and a small number of floors below it. A typical construction cycle using three levels of shores is illustrated in Figure 8.1.

In discussing construction loads, it is convenient to express them as a factor times the sum of the self-weight of the floor and the dead load of the formwork. The term **floor loading ratio** is used for this factor. Progressive slab deflections that had been causing problems in Sweden in the early 1950s led to the first study by Nielsen (1952) of a rational approach to stripping formwork for floors. Nielsen gave a detailed analysis of the distribution of load between a system of connected shores and floor slabs. The method considered the deformation characteristics of both the slabs and the shores. The maximum load ratio obtained by Nielsen on a slab assuming three levels of shores was 2.56. Grundy and Kabaila (1963) developed a simplified method of analysis for floor loads based on the following assumptions:

1. The slabs behave elastically.
2. Initially, the slabs are supported from a completely rigid foundation.
3. The shores supporting the slabs and formwork may be regarded as a continuous uniform elastic support, the elastic properties of which may be expressed by a coefficient K, where K is the load intensity that produces unit deformation of the support.
4. Any added load is distributed among the supporting slabs in proportion to their relative flexural stiffnesses.

Grundy and Kabaila assumed that K was infinite and carried out their analyses assuming a constant flexural stiffness for all connected slabs, as well as a flexural stiffness increasing with age. It was found that the error introduced by assuming equal relative stiffnesses for the floors is not appreciable.

Figure 8.2 represents the construction of a multifloor building using three levels of shores (and forms) for a 7-day casting cycle, with stripping in 5 days. The loads carried by the slabs and the shores, in terms of the loading ratio, are indicated on the figure adjacent to the element concerned. Floors 1, 2, and 3, supported from the ground by stiff shores, cannot deflect and therefore carry no load; all the load is carried by the shores directly to the foundation. At the age of 26 days, the lowest level of shores is removed, allowing all three slabs to deflect and carry their self-weight. The removed shores are placed on the third floor slab and the fourth floor is poured. As all three supporting slabs have equal stiffness, the weight of the newly poured slab is carried equally by the three lower slabs. The absolute maximum load ratio occurs when the shores connecting the supporting assembly with the ground level are removed; however, the load ratio converges for upper floor levels. For the same structure considered by Nielsen, Grundy

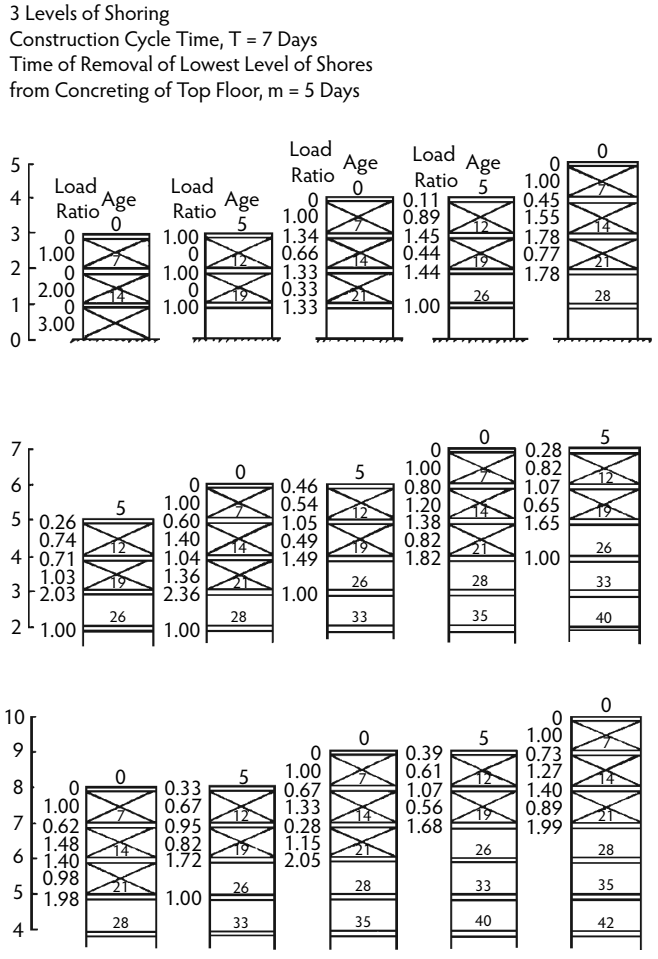

FIGURE 8.2 Load ratio vs. time for three levels of shores.

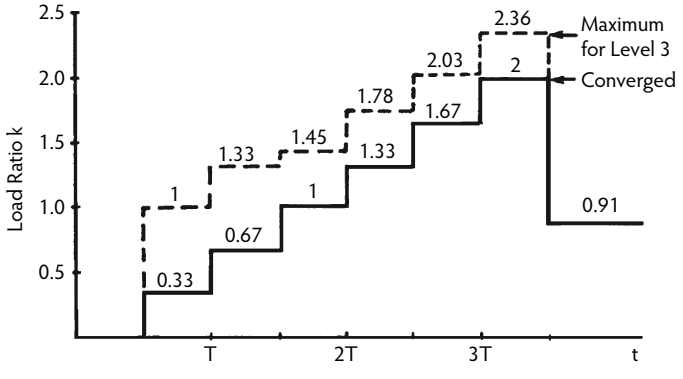

FIGURE 8.3 Load-ratio history for three levels of shores.

and Kabaila obtained an absolute maximum load ratio of 2.36, while the converged value for upper floor levels was 2.00 (Figure 8.2). The most heavily loaded slab is always the last slab that is supported directly from the foundation. The load time histories of the third floor slab and a typical slab are shown in Figure 8.3. Altering the number of shored levels has little effect on the maximum load ratio value; however, by

TABLE 8.1 Floor-Loading Ratio

Author	Maximum Value (Converged Values in Brackets) $m = 2$	$m = 3$	$m = 4$	$m = 5$	Comment
Nielsen (1952)	2.17 2.0Δ	2.28× 2.56+	—	—	Values for floor level 2 only; ×, timber props; +, steel props ($n = 1$); Δ, observed
Grundy and Kabaila (1963)	2.25 (2.00)	2.36 (2.00)	2.43 (2.00)	—	$n = 5$
Beresford (1964)	2.25	(2.00)* (2.06)* 2.35 (2.32)	2.45	2.50	* Obtained for rapid hardening, normal and slow maturing concretes, respectively ($n = 5$)
Blakey and Beresford (1965)	2.25 2.25+	2.3	—	—	+, Stepwise construction
Beresford (1971)	—	2.2 1.5Δ	—	—	$n = 4$; Δ, observed

Note: Here m = number of levels of shoring used and n = time in days for removal of lowest levels of shores after concreting top floor.
Source: Adapted from Wheen, R.J., *Concrete Int.*, 4(5), 56–62, 1982.

decreasing the number of shored levels, the age of the slab at which the maximum ratio occurs also decreases. Beresford (1964) used infinite as well as various finite values of K (see assumption 3 above) and found that the results of floor-load analysis were not appreciably affected.

In addition to variations in moduli of elasticity due to concrete age, cracking of slabs occurring during construction affects the distribution of loads among slabs in the supporting assembly. Sbarounis (1984) reported that incorporating the effects of cracking into the load distribution factors for the supporting slabs reduced the previously calculated maximum load ratios by approximately 10%. Blakey and Beresford (1965) recommended a stepped sequence of construction in a system of floors and shores as a means of controlling the construction loads imposed on both the slabs and the shores. The advantage of this method lies in the fact that a young slab is given more time to develop adequate strength before the application of construction load from the casting of a new slab directly above. Table 8.1, adapted from Wheen (1982), shows clearly that all writers on the subject agree that floor loading ratios during construction usually exceed values of 2.

The sequence of construction illustrated in Figure 8.1 uses three sets of forms. Economic considerations usually necessitate the removal of formwork as soon as possible for reuse. This necessity has given rise to the widespread practice of *reshoring*. The reshoring technique typically involves using only one level of forms or shores and several levels of reshores. Basically, the forms or shores are removed from beneath a slab, allowing it to deflect and carry its own weight; reshores are then installed, allowing the load during subsequent concrete placement to be shared between the various slabs in the supporting assembly. At the time of installation, reshores carry no significant load. Figure 8.4 illustrates a construction scheme with two levels of shoring and one level of reshoring.

Agarwal and Gardner (1974) in Canada and Marosszeky (1972) in Australia analyzed the loads imposed on slabs using the shoring/reshoring method of construction and utilizing the same simplifying assumptions as used earlier by Grundy and Kabaila (1963). The slab loads when using two levels of shores and one level of reshores are calculated as shown in Figure 8.5. The time history of slab loads using two levels of shores and one level of reshores is shown in Figure 8.6.

Taylor (1967) suggested a technique of stripping formwork to reduce the loads imposed on a slab during construction. By slackening and tightening adjustable shores before each new slab is cast, the loads distributed to the shores and slabs are reduced considerably. With this method, all shores at one level must be slackened simultaneously; thus, it requires greater supervision and inspection. Taylor reported that the maximum load ratio was reduced from the 2.36 obtained by Grundy and Kabaila to a

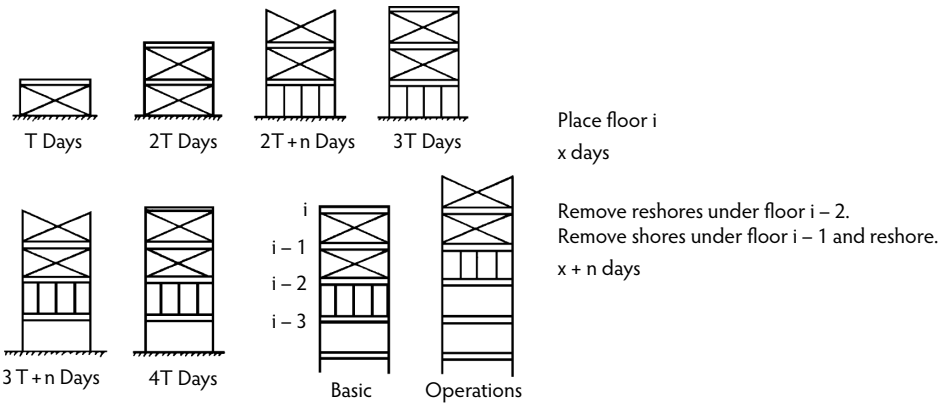

FIGURE 8.4 Construction sequence using two levels of shores and one level of reshores.

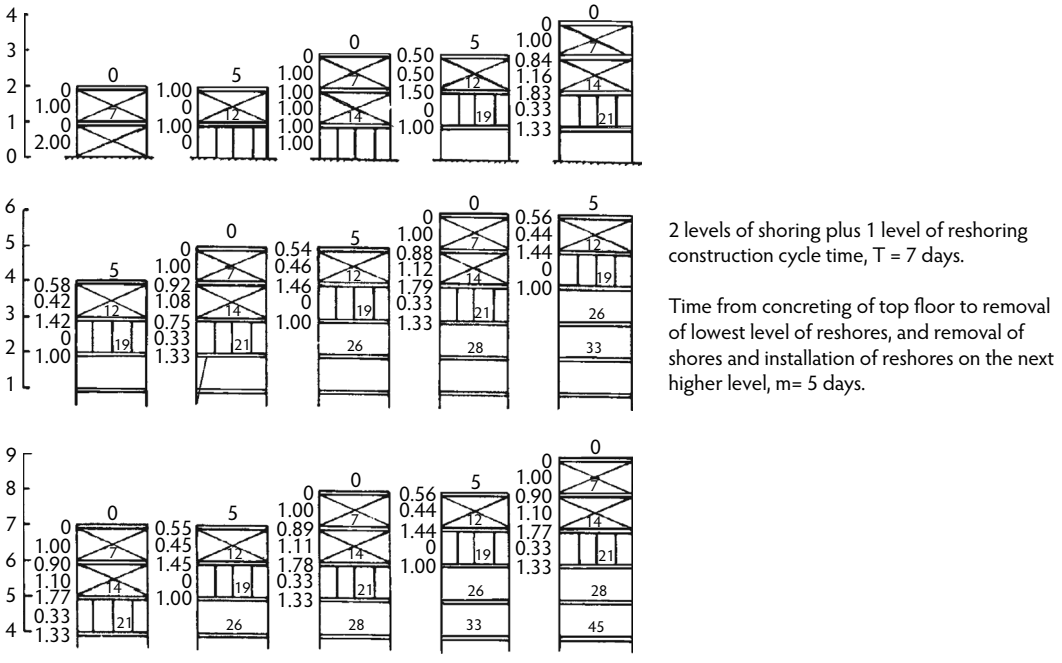

FIGURE 8.5 Load ratio vs. time for two levels of shores and one level of reshores.

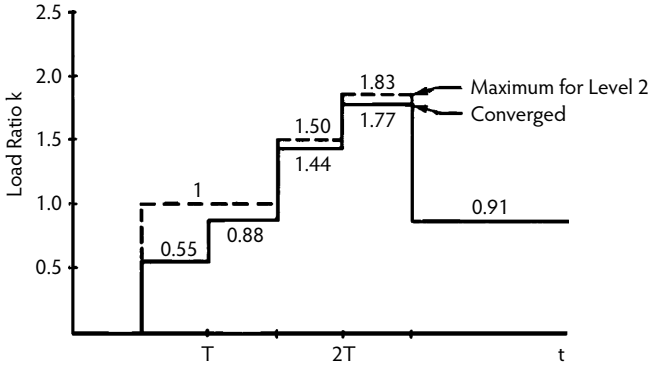

FIGURE 8.6 Load-ratio history for two levels of shores and one level of reshores.

TABLE 8.2 Theoretical Maximum Load Ratios on Floor and Prop for Various Shore/Reshore Combinations

	Absolute Maximum Load Ratio		Converged Maximum Load Ratio	
Shore + Reshore	On Floor Slab	On Prop	On Floor Slab	On Prop
1 + 1	1.50	1.0	1.50	1.0
1 + 2	1.34	1.0	1.34	1.0
1 + 3	1.25	1.0	1.25	1.0
1 + 4	1.20	1.0	1.20	1.0
1 + 5	1.17	1.0	1.17	1.0
2 + 0	2.25	2.0	2.00	1.0
2 + 1	1.83	2.0	1.78	1.11
2 + 2	1.75	2.0	1.67	1.17
2 + 3	1.61	2.0	1.60	1.21
2 + 4	1.60	2.0	1.56	1.25
2 + 5	1.55	2.0	1.53	1.24
3 + 0	2.36	3.0	2.00	1.34
3 + 1	2.10	3.0	1.87	1.37
3 + 2	1.97	3.0	1.80	1.40
3 + 3	1.84	3.0	1.76	1.42
3 + 4	1.77	3.0	1.72	1.43
3 + 5	1.77	3.0	1.70	1.43

Source: Lasisi, M.Y. and Ng, S.F., *Concrete Int.*, 1(2), 24–29, 1979.

value of 1.44. Taylor's method is the same in principle as stripping and immediate reshoring of a slab. Marosszeky (1972) described complete release and reshoring of a floor slab such that the floor carried its own dead weight at a time $(T - 1)$ days, where T is the construction cycle of floors. This reshoring technique produces less construction load on the supporting slabs and props when compared with using undisturbed shores.

Although the load ratios previously defined reflect the slab-plus-formwork dead weights, a construction live load is also present. Whereas the dead load can be estimated with reasonable certainty, the live loads can vary significantly depending on the construction method used to place concrete. ACI Committee 347 (2004) recommends that the design live load should be at least 50 psf (2.4 kPa) of the horizontal projection. A comprehensive study (Fattal, 1983) on construction loads in concrete buildings indicated that, when concrete is placed by a bucket, the live load may be as high as 40 to 50 psf (1.9 to 2.4 kPa). On the other hand, the American National Standards Institute (ANSI) Standard A10.9 (1997) does not provide a numerical value and leaves the determination of live load to the formwork designer; however, the standard does list factors to be considered in estimating the design load, such as the weight of workers, equipment, runways, and impact of concrete.

Hurd (2005) has suggested a minimum construction live load of 50 psf (2.4 kPa) for designing forms. Lasisi and Ng (1979) presented a method to include the live-load effect. For a typical flat-plate structure, assuming a supporting assembly of two shore levels plus one reshore level, a construction live load of 50 psf (2.4 kPa) removed after the casting day, and a constant modulus of elasticity for the connected slabs, the absolute maximum load ratio would increase 9% over that predicted by Grundy and Kabaila (1963). Both Agarwal and Gardner (1974) and Sbarounis (1984) accounted for the construction live-load effect by increasing the maximum load carried by the lowest slab in the supporting assembly. Sbarounis recommended additional loads, due to a 50-psf (2.4-kPa) live load, of $55/N$ and $35/N$ psf ($2.6/N$ and $1.7/N$ kPa) for uncracked and cracked slabs, respectively, with N representing the total number of levels in the supporting assembly.

Table 8.2 shows absolute maximum and converged maximum load ratios on slabs and supporting props for various combinations of levels of shores and reshores. Table 8.2 and Figure 8.6 indicate that the use of two levels of shoring and one level of reshoring, rather than three levels of shores, reduces the

TABLE 8.3 Comparison of Construction Loads with Service Loads

Construction Loads (psf)		Service Loads (psf)	
8-in. slab	100	8-in. slab	100
Formwork	10	Ceiling and mechanical	15
Subtotal	110	Partitions	20
		Live load	50
		Total (after 28 days)	185
Load Ratio			
3 Level of Shores		2 Levels of Shores Plus 1 Level of Reshores	
1.00 at 5 days	110	1.00 at 5 days	110
1.34 at 7 days	147	1.00 at 7 days	110
1.45 at 12 days	160	1.50 at 12 days[b]	165
1.78 at 14 days	196	1.83 at 14 days	201
2.03 at 19 days	223[a]	1.00 at 19 days	110
2.36 at 21 days	260		
1.00 at 26 days	110		

[a] Deflection not restrained beyond 19 days.
[b] Allowed to deflect under these construction loads at 12 days. Further deflections partly restrained for the next 7 days.

absolute maximum load ratio from 2.00 to 1.78. This is advantageous in most situations, although with reshoring the maximum load ratios come into play at an earlier age than with shoring, as should be apparent from Figure 8.2 and Figure 8.5. Table 8.3 presents construction loads for floor 3, which experiences the absolute maximum load ratio. The construction loads are compared with the design service loads in the table. It is clear that the construction loads are more critical than the design loads. Also important, construction loads act on concrete that has not attained the age at which it is supposed to experience design service loads.

8.2.2 Field Verification

Agarwal and Gardner (1974) used field measurements to check the accuracy of various analysis methods for estimating the shore and slab load distribution. Their investigation consisted of directly measuring the load ratios applied to shores and reshores during construction and determining the loads carried by the floor slabs at different stages of construction. The shore and reshore loads for two buildings were measured: Alta Vista Towers in Ottawa, Ontario, Canada, and Place du Portage in Hull, Quebec, Canada. Steel shores were used for both structures. Three levels of shores and four levels of reshores were used to temporarily support the flat-slab floors in the construction of the 22-story Alta Vista Towers. Measurement of the shore and reshore loads, for the shore and reshore arrangements shown in Figure 8.7, was limited to the 7th through the 13th stories. Three levels of shores and no reshores were used in the construction of the 27-story Place du Portage structure, which is a flat-slab office building. The shoring arrangement is shown in Figure 8.8. Measurements were taken from the 19th through the 22nd stories.

According to Liu et al. (1985a), three factors concerning the field measurement data should be noted:

1. Field measurements were not taken from the ground level, so the actual slab and shore loads of the entire system during construction were not available.
2. Typical shores and reshores chosen for instrumentation were located in the central portions of the slabs (Figure 8.7 and Figure 8.8); thus, the influence of the surrounding boundary beams and columns was less pronounced. From the measured data reported in Agarwal and Gardner (1974),

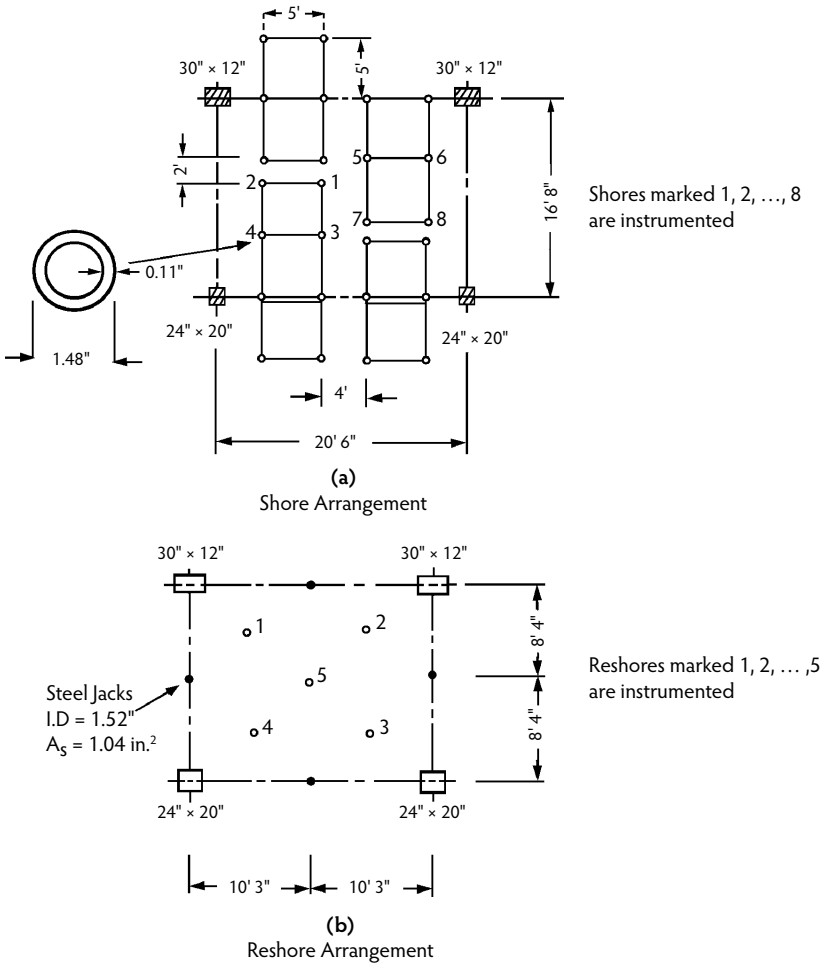

FIGURE 8.7 (a) Shore and (b) reshore arrangements for Alta Vista Towers. (From Agarwal, R.K. and Gardner, N.J., *ACI J.*, 71(11), 559–569, 1974.)

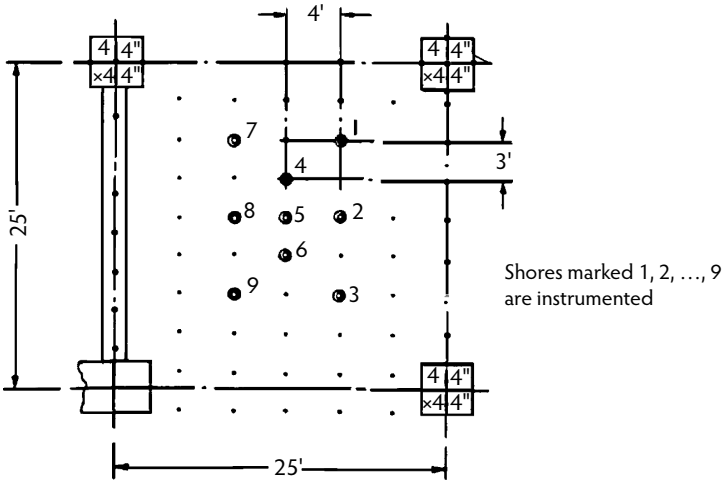

FIGURE 8.8 Shoring arrangements for Place du Portage. (From Agarwal, R.K. and Gardner, N.J., *ACI J.*, 71(11), 559–569, 1974.)

the coefficient of variation of the shore axial force varied from 0.04 to 0.23, depending on the distance of the shore from the boundary line.

3. The values of the modulus of elasticity of concrete (E_c) and the shore height were not reported in Agarwal and Gardner (1974). Without these, it is not possible to use the measured shore-load data to check other methods further.

Comparisons between field measurements for both buildings and the slab and shore loads given by the simplified analysis of Grundy and Kabaila (1963) are reported in Agarwal and Gardner (1974). To check the assumptions of equal slab stiffness originally used by Grundy and Kabaila, the slab shore loads were calculated by both using equal slab stiffnesses and varying the slab stiffness for each floor to account for an increase in E_c with age. Table 8.4 shows the comparison of field measurements for each story in both buildings to the calculated maximum slab and shore loads.

Good agreement between the predictions of simplified analysis and the field measurements was generally observed. Uses of variable slab stiffnesses in the simplified analysis produced closer agreement: The maximum discrepancy for variable slab stiffness was less than 10%, but for constant slab stiffness it was as high as 16%. Further, it was shown in Agarwal and Gardner (1974) that the calculated results based on either constant or variable slab stiffnesses consistently predicted the correct construction step and the location of the maximum shore and slab loads.

Lasisi and Ng (1979) carried out measurements on 5 regular floors to investigate peak construction loads on slabs, shores, and reshores in a 15-story flat-slab office building in Ottawa, Canada. One level of shores and two levels of reshores were utilized in construction. The period between the casting of a slab section and the next slab directly above was 10 days on average. The forms were supported on tubular steel shores. Reshores were made of telescopic steel jacks. The average stripping time for a slab in the instrumented section of the building was 5 days. Measurement on this building was commenced during concreting of the 7th-floor slab and continued until after the stripping of the 11th floor. An interior bay of a section of the building was instrumented. Load cells were installed beneath a shore or a reshore at the chosen location; the instrumented reshore on each level was vertically below the load cell placed underneath the scaffold shore.

Shore and reshore loads were calculated by Lasisi and Ng (1979) using Grundy and Kabaila's simplified analysis, taking into consideration the presence of 50 psf (2.4 kPa) of construction live load during concrete placement. As can be seen from Table 8.5, there was reasonably close agreement between measured and theoretical maximum shore loads; however, the loads measured on the reshores were found to be on average considerably less than the corresponding theoretical values.

8.2.3 Refined Analysis

Liu et al. (1985a) carried out refined analysis to determine shore and slab load distribution, considering the actual rigidity of shores and the time-dependent variation in slab stiffness due to concrete maturity. Their refined analysis technique treated the shore–slab interaction as a two-dimensional problem and was based on the following assumptions:

1. The slabs behave elastically and their stiffnesses are time-dependent.
2. The shores and reshores behave as continuous uniform elastic supports, and their axial stiffnesses are finite and time-independent.
3. The foundation is rigid.
4. The joints between the shores and slabs are pinned connections.
5. The slab edges are either fixed or simply supported.

Comparison of maximum loads computed by the simplified Grundy–Kabaila method (1963) with those predicted by the refined method indicated that the maximum relative differences in the two methods varied between –5 and +9%. Because the effect of shore stiffness was not considered, the calculated results using the simplified method showed larger errors (deviations from field measurements) than the results

TABLE 8.4 A Comparison between Field Measurements and Calculated Maximum Slab and Shore Loads

		Maximum Slab Load ÷ Slab Weight					Maximum Shore Load ÷ Slab Weight				
		Field Measurement	Calculation with E_c Constant	Calculation with E_c Variable	Comparisons		Field Measurement	Calculation with E_c Constant	Calculation with E_c Variable	Comparisons	
Building	Level	(1)	(2)	(3)	(2)/(1)	(3)/(1)	(4)	(5)	(6)	(4)/(5)	(4)/(6)
Alta Vista Towers	7	1.88	1.72	1.83	0.91	0.97	1.65	1.40	1.58	0.85	0.96
	8	1.93	1.70	1.85	0.88	0.96	1.51	1.46	1.57	0.97	1.04
	9	1.91	1.72	1.74	0.90	0.91	1.70	1.42	1.58	0.84	0.93
	10	2.02	1.72	1.99	0.85	0.99	1.37	1.43	1.46	1.04	1.07
	11	1.07	1.13	0.99	1.06	0.93	1.68	1.44	1.62	0.89	1.00
	12						1.64	1.43	1.61	0.87	0.98
Mean					0.92	0.95				0.90	1.00
Standard deviation					0.08	0.03				0.09	0.05
Place du Portage	19	2.11		2.11		1.00	1.48		1.41		0.95
	20	1.34		1.30		0.97	1.44		1.44		1.00
	21						1.45		1.41		0.97
Mean						0.99					0.97
Standard deviation						0.02					0.03

Source: Taylor, P.J., *Australian Civil Eng. Const.*, 8(2), 31–35, 1967.

TABLE 8.5 Measured Construction Loads on Shores and Reshores

Shore or Reshore Resting on Level	Construction Operation		Imposed Loads		
	A (Concreting)	B (After Stripping and Reshoring)	psf	Load Ratios	Theoretical Load Ratios
4	A-7R	—	50.1	0.40	0.47
5	A-7R	—	77.0	0.62	0.93
	—	B-7R	5.0	0.04	0
6	A-8R	—	13.4	0.11	0.47
	A-7S	—	154.0	1.23	1.40
	—	B-7	—	—	—
	A-8R	—	97.3	0.78	0.93
	—	B-8R	8.9	0.07	0
7	A-9R	—	17.6	0.14	0.47
	A-8S	—	188.8	1.51	1.40
	—	B-8	—	—	—
	A-9R	—	106.4	0.85	0.93
	—	B-9R	21.1	0.17	0
8	A-10R	—	40.1	0.32	0.47
	A-9S	—	209.5	1.68	1.40
	—	B-9	—	—	—
	A-10R	—	110.9	0.89	0.93
	—	B-10R	9.4	0.08	0
9	A-11R	—	28.2	0.23	0.47
	A-10S	—	135.6	1.09	1.40
	—	B-10	—	—	—
	A-11R	—	59.9	0.48	0.93
	—	B-11R	23.3	0.19	0
10	A-11S	—	182.5	1.46	1.40
	—	B-11	—	—	—

Note: S, shore; *R*, reshore.
Source: Lasisi, M.Y. and Ng, S.F., *Concrete Int.*, 1(2), 24–29, 1979.

predicted using the refined method. The simplified Grundy–Kabaila method reliably predicted the construction step and location where the maximum slab and shore loads would occur but generally underestimated the actual load ratios; consequently, the maximum slab and shore loads predicted by the simplified method could be corrected using a modification coefficient. Liu et al. (1985a) recommended that the value of the modification coefficient for the simplified method vary from 1.05 to 1.10 for design purposes.

Liu et al. (1985b) also used a more realistic three-dimensional (3-D) model to check the approximation of the Grundy–Kabaila simplified method and the two-dimensional (2-D) refined method (Liu et al., 1985a). A number of simplifying assumptions were made when they conducted the refined 3-day analysis. First, the reinforced concrete slabs were assumed to behave elastically; their stiffnesses were taken as time dependent; slab edges were either free or rotationally fixed (but free to deflect). Second, the vertical deflections of the slabs at the slab–column joints were neglected. Third, the weight and structural details of each floor were assumed to be similar. Fourth, the shores and reshores were presumed to be continuous ideal elastic supports with equal axial stiffnesses; the joints between the shores and the slabs were assumed to be pin-ended connections. Finally, the foundation was assumed to be rigid and unyielding. The influences of foundation rigidity, column deformation, and slab aspect ratio were examined using the 3-day model.

On the basis of the various factors examined for the 3-day model, the following conclusions and observations were made:

1. The maximum slab loads given by the 2-day refined analysis and the 3-day refined analysis were nearly identical. The maximum shore load increased slightly for the 3-day refined analysis.
2. Variations of the foundation rigidity affected slab displacements more than the maximum shore loads and slab moments. When the rigidity of the foundation decreased, the maximum slab moments and the maximum shore loads decreased.
3. The vertical deformation of columns could be neglected when computing the maximum shore loads and slab moments.
4. A change in the slab aspect ratio produced very little increment in the maximum shore load for slabs with free edges. For a slab with fixed edges, the total increment of the maximum shore load was 3% for the aspect ratios examined (between 0.6 and 1.0).

In all cases examined, a modification coefficient that varied from 1.05 to 1.10 could be used to conservatively correct the results of the Grundy–Kabaila simplified method. It was found that nonuniform distribution of shore stiffnesses did not change the prediction of the construction step and location where the maximum slab moments and shore loads occurred.

Stivaros and Halvorsen (1990) questioned the good agreement mentioned earlier between the simplified Grundy–Kabaila method and existing field measurements. They pointed out that, in actual building cases investigated (Agarwal and Gardner, 1974; Lasisi and Ng, 1979), steel shoring systems had been used, justifying the Grundy–Kabaila assumption of infinite shoring system stiffness. The fact that the field measurements were observations around the center of the slab and thus ignored the influence of structural continuity contributed to the good agreement between field data and the theoretical values. Another important fact was that field measurements were not taken from the ground level, so the complete loading–unloading construction cycle was not recorded.

Stivaros and Halvorsen (1991) also pointed out that most practical methods for analyzing construction loads have employed single-bay idealizations of frames. This is a definite limitation to the proper evaluation of the punching shear forces that are the critical load effect in most flat-slab systems. A single-bay structural idealization cannot fully assess the maximum shear force effects at the columns from both direct shear forces and unbalanced moments; therefore, a practical and simple method that took into account the continuity of concrete structures over several bays, as well as the interaction of the floor slabs and the shoring system over several stories, was thought to be needed.

The *equivalent frame method* (EFM) of analysis was found by Stivaros and Halvorsen (1990) to be a reasonable procedure for accomplishing the preceding goal. The EFM was first developed as a viable procedure for analyzing reinforced concrete slab systems, particularly for the effects of gravity loads. It has been applied to lateral load analysis of slab systems, as well. A computer program was developed for the study to determine the construction load distribution among the slabs and the shoring system during the construction of multistory buildings. A multistory building under construction is modeled according to the assumptions of the equivalent frame method as described in ACI Committee 318 (2005). A schematic representation of an idealized structure is shown in Figure 8.9. The shores and reshores are replaced by an equal number of elastic supports, each having a stiffness equal to the total stiffness of the corresponding shores. It is assumed that the reshores carry no load at the time of installation. The load of the freshly cast concrete is applied to the top-floor shores as concentrated loads. The load is shared among the shores according to their tributary areas. The connection between the shores or reshores and the floor slabs can be reasonably assumed to be pin-jointed. At ground level, shores and reshores are assumed to be supported on a rigid foundation. The EFM concepts are applied to determine the frame member stiffness coefficients. The idealized two-dimensional frame is then analyzed elastically using conventional stiffness analysis procedures to determine the member forces, including the axial load on the shoring system.

A typical floor plan of the equivalent frame used by Stivaros and Halvorsen (1990) for parametric studies is shown in Figure 8.10. The shores and reshores are idealized as series of vertical truss-type elements, each with a stiffness equivalent to the total stiffness of the shores or reshores on the row it

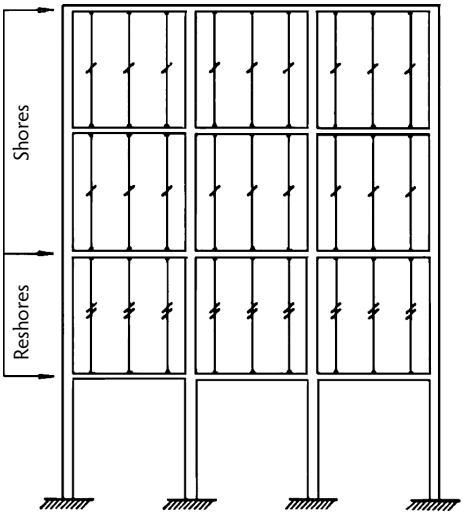

FIGURE 8.9 Structural idealization. (From Stivaros, P.C. and Halvorsen, G.T., *Concrete Int.*, 13(8), 57–62, 1991.)

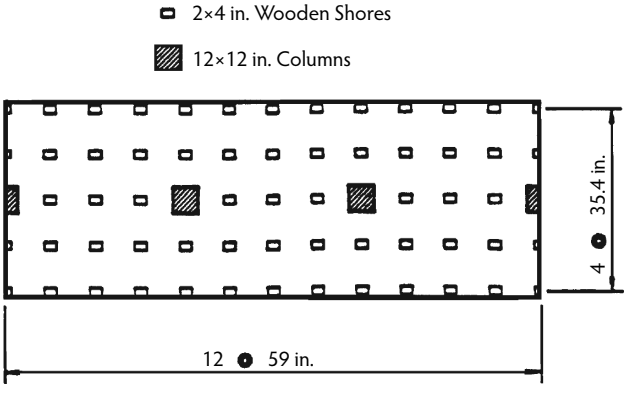

FIGURE 8.10 Typical plan of equivalent frame studied by Stivaros and Halvorsen. (From Stivaros, P.C. and Halvorsen, G.T., *ACI Struct. J.*, 87(5), 589–596, 1990.)

represents. Two levels of shores and one level of reshores were assumed, with a construction rate of one floor per week. Only the slab dead load was considered in analysis. The loads in slabs were normalized to the self-weight of each slab, and the loads on shores were normalized to the weight of the slab supported by the shores. The construction operations were denoted with a set of two numbers. The first number represented the number of the floor level under construction, and the second indicated the phase of construction (Figure 8.11). The numeral 1 indicated casting of the top floor, 2 denoted the removal of lower level of reshores, and 3 indicated the removal of the lower level shores; for example, "Operation 3-2" referred to the maximum slab or shore loads during removal of the lower level of reshores after casting the third floor. The maximum slab loads evaluated using the EFM, both multi-bay and single-bay models, along with the corresponding results of the simplified Grundy–Kabaila method and results by Liu et al., are plotted in Figure 8.12 with respect to the sequential construction operations. The results reported for the EFM multi-bay model are those for an interior bay.

Figure 8.13 and Figure 8.14 show the variation of the maximum slab load with respect to the number of reshored levels for both the equivalent frame model and the simplified method for one level and two levels of shoring, respectively. As the figures show, the EFM and the simplified method diverge as the number of reshored levels increases. As the number of shored levels increases (comparing both figures), the diversion of the EFM from the simplified method slows. Figure 8.14 shows that the combination of

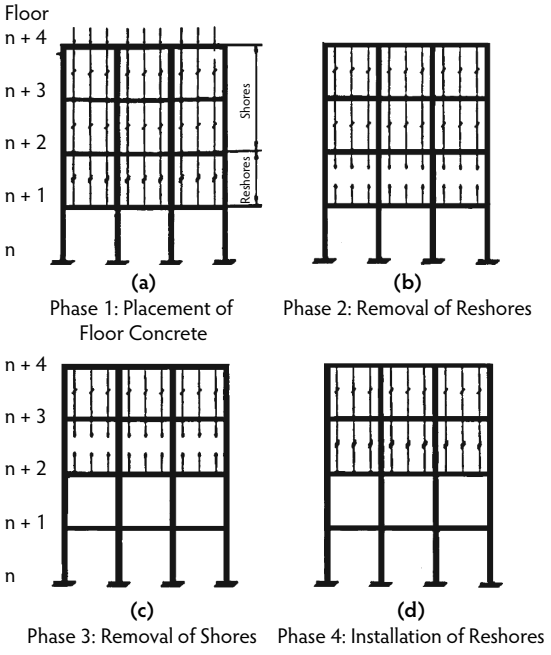

FIGURE 8.11 Construction phases. (From Stivaros, P.C. and Halvorsen, G.T., *Concrete Int.*, 14(8), 27–32, 1992.)

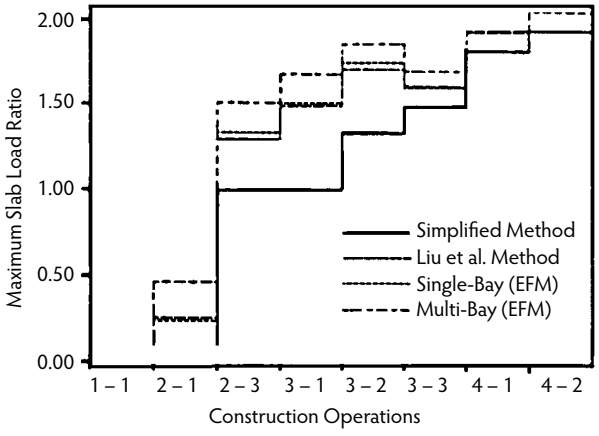

FIGURE 8.12 Comparison of methods of construction load analysis. (From Stivaros, P.C. and Halvorsen, G.T., *ACI Struct. J.*, 87(5), 589–596, 1990.)

two shored levels and one reshored level (the combination used by Liu et al.) is a case where the EFM and the simplified method converge with a difference of about 5%. The difference increases as the number of reshored levels increases, approaching 15% when three reshored levels are used. Considering the case of the one-shore scheme with four reshored levels from Figure 8.13, the difference between the two methods is about 30%.

Figure 8.15 shows the variation of the maximum slab load with respect to the number of reshored levels for one level of shoring and for both the single-bay and multi-bay models. As can be seen, the two methods diverge as the number of reshored levels increases. The multi-bay model always predicts higher maximum slab loads than the single-bay model, with differences as great as 14% in the case of three reshored levels.

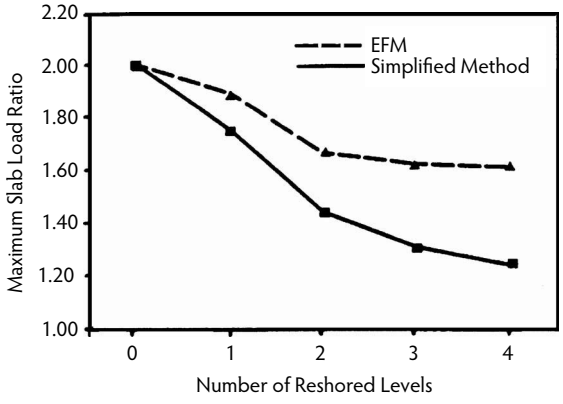

FIGURE 8.13 Comparison of EFM and simplified method: one shored level. (From Stivaros, P.C. and Halvorsen, G.T., *ACI Struct. J.*, 87(5), 589–596, 1990.)

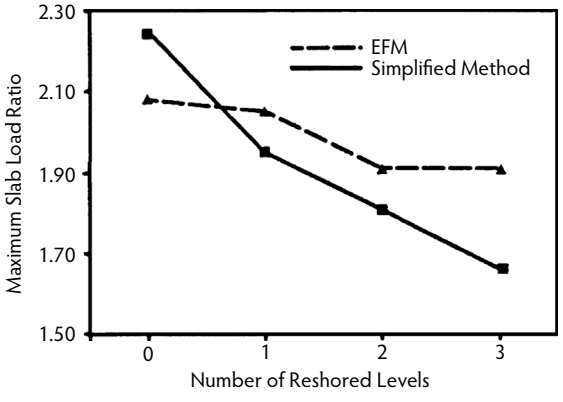

FIGURE 8.14 Comparison of EFM and simplified method: two shored levels. (From Stivaros, P.C. and Halvorsen, G.T., *ACI Struct. J.*, 87(5), 589–596, 1990.)

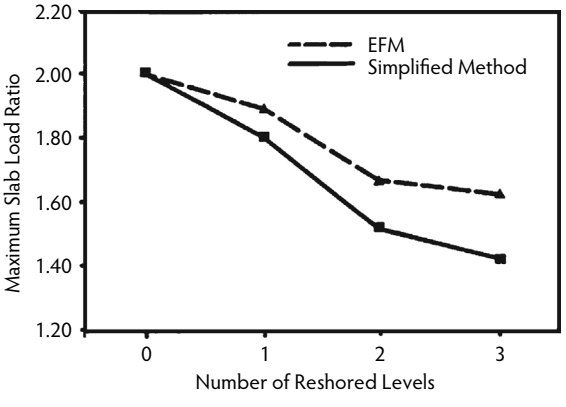

FIGURE 8.15 Comparison of single-bay and multi-bay models: one shored level. (From Stivaros, P.C. and Halvorsen, G.T., *ACI Struct. J.*, 87(5), 589–596, 1990.)

The stiffness of the shoring system affects the behavior of both the single-bay and multi-bay models. Figure 8.16 shows the variation of the maximum slab load of the first floor during the casting of the third floor with respect to the shoring system stiffness for both models. The stiffness of the shoring system varies

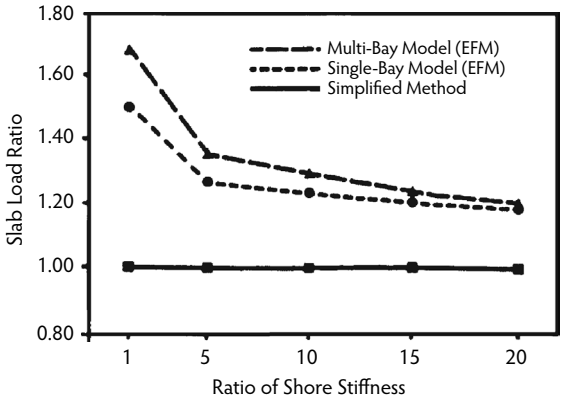

FIGURE 8.16 Comparison of analytical models based on shoring system stiffness. (From Stivaros, P.C. and Halvorsen, G.T., *ACI Struct. J.*, 87(5), 589–596, 1990.)

in five increments from the actual value to 20 times the actual value. As the figure shows, the multi-bay model predicts higher values than the single-bay model. As the stiffness of the shoring system increases, both methods tend to converge. When the stiffness reaches a relatively infinite value, both methods produce almost identical results approaching the simplified method. The multi-bay model is more advantageous than the single-bay model because it represents the concrete structure as a more realistic monolithic continuous frame. Furthermore, it can provide information about the total shear force (due to the gravity load and the unbalanced moments) applied to slab–column joints. Considering the advantages that multi-bay analysis offers, it is preferable to apply the more realistic continuous multi-bay model when possible.

To investigate the influence of slab stiffness, the construction example was analyzed for two construction cycles of 3 and 7 days. The percentages of the 28-day concrete strength for the 3- and 7-day cycles were determined using the maturity concept. The age of the slab at which the maximum load occurred differed for the two construction schedules. Figure 8.17 shows the maximum slab loads with respect to the slab age in days for the 3- and 7-day construction rates. Despite the fact that both schedules predict almost identical maximum slab loads, the ages of the slabs under these loads are different. The maximum load of 2.08 times the slab self-weight for the 3-day schedule occurred on a 7-day-old slab, whereas the maximum load of 2.06 times the slab self-weight for the 7-day schedule occurred on a 19-day-old slab.

The presence of drop panels around the columns or beams between columns can significantly increase the stiffness of slabs and columns. To determine the influence of drop panels and beams, the construction example was analyzed for two additional conditions. The first condition assumes beams spanning between columns in both directions, with an overall depth of 20 in. (510 mm) and width of 12 in. (300 mm). The second condition assumes a type of flat-slab construction with square drop panels around columns with depth equal to half the slab thickness of 7.1 in. (180 mm) and length equal to one third the 236-in. (6000-mm) span. Figure 8.18 compares the results of the cases with and without beams or drop panels. The slabs with beams or drop panels share higher loads than the flat-plate slab because the beams and the drop panels increase the stiffness of the slab. A similar construction load distribution occurs when the slab thickness and, consequently, the slab stiffness are increased. The degree of influence of beams, drop panels, or the slab thickness on the construction load distribution is totally dependent on the size of these structural members relative to the global size of the equivalent frame as well as on the stiffness of the shoring system. If the stiffness of the shoring system is infinite relative to the stiffness of the supported slabs, the effect of the slab stiffness variation on the load distribution will be minimal.

To determine the influence of the axial shore stiffness on the load distribution, the construction example was investigated by increasing the shoring system stiffness by 5 increments up to 20 times the actual value. The slab stiffness and the number of shores or reshores per bay were kept constant for this analysis, the results of which are shown in Figure 8.19. As can be seen, the shoring stiffness has a

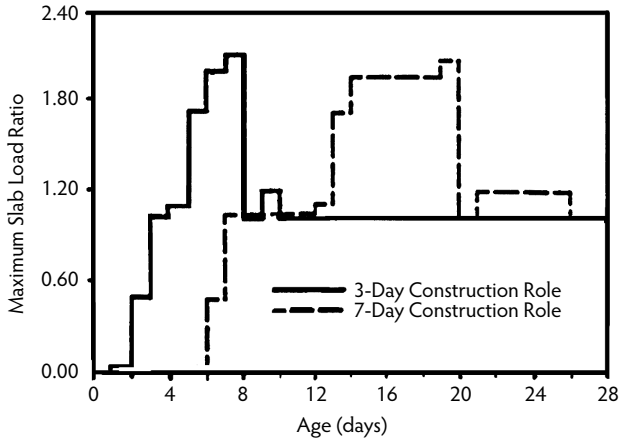

FIGURE 8.17 Comparison of construction rates. (From Stivaros, P.C. and Halvorsen, G.T., *ACI Struct. J.*, 87(5), 589–596, 1990.)

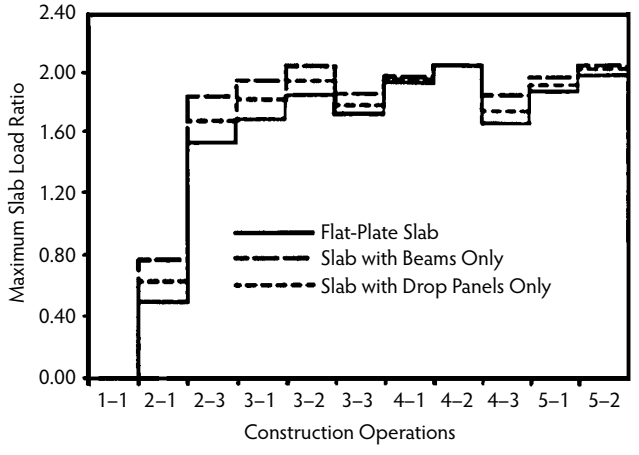

FIGURE 8.18 Comparison of slab types. (From Stivaros, P.C. and Halvorsen, G.T., *ACI Struct. J.*, 87(5), 589–596, 1990.)

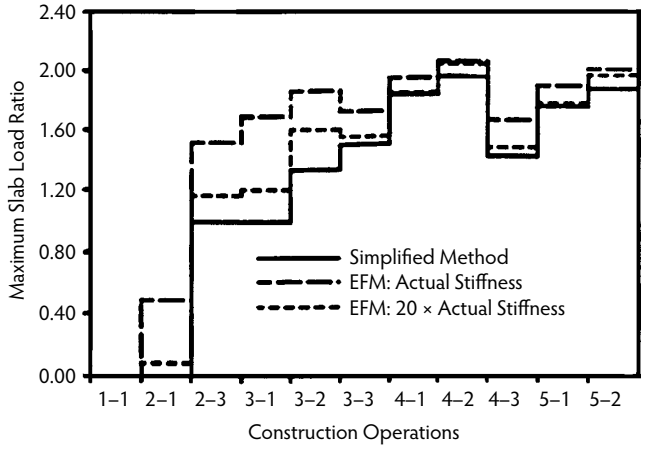

FIGURE 8.19 Comparison of shoring system stiffnesses. (From Stivaros, P.C. and Halvorsen, G.T., *ACI Struct. J.*, 87(5), 589–596, 1990.)

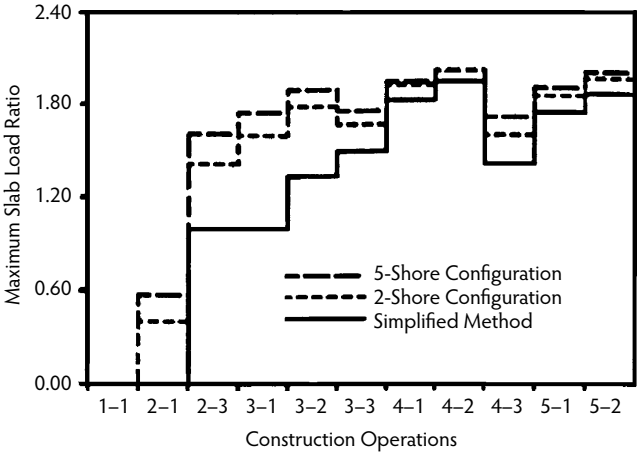

FIGURE 8.20 Comparison of shoring configuration types. (From Stivaros, P.C. and Halvorsen, G.T., *ACI Struct. J.*, 87(5), 589–596, 1990.)

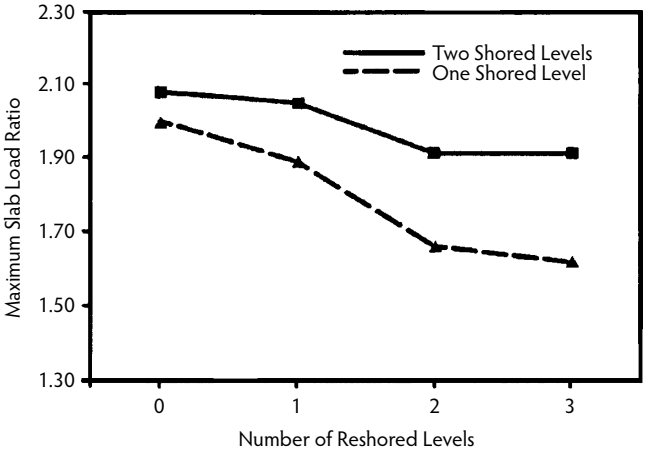

FIGURE 8.21 Influence of the number of reshored levels on the maximum slab load. (From Stivaros, P.C. and Halvorsen, G.T., *ACI Struct. J.*, 87(5), 589–596, 1990.)

considerable influence on the construction load distribution. The difference in the slab load, for example, is up to 40% during Operation 3-1. Figure 8.19 also incorporates the values predicted by the simplified method and illustrates how the shoring system stiffness affects the slab load during construction. An important observation from Figure 8.19 is that, as the stiffness of the shoring system approaches infinity, the predicted maximum slab loads using the EFM draw near the loads predicted by the simplified method. This clearly shows that the differences of the equivalent frame method and the simplified method are very much due to the shoring system stiffness.

It has been common practice to consider the shores to be spaced closely enough that shore reactions can be treated as uniformly distributed. This may not be true when a flying-truss forming system is used. To determine the effects of various shoring systems, the construction example was investigated using two, three, four, and five shores in each bay. The total stiffness of shores and reshores in each bay was kept constant for all cases and was evenly distributed among the shores and reshores. The slab stiffness was also kept constant. As can be seen from Figure 8.20, the two-shore-per-bay configuration predicts lower values than the five-shore configuration throughout the construction, despite the fact that the total stiffness of the shoring system is the same for both cases. The fewer the number of shores per bay, the

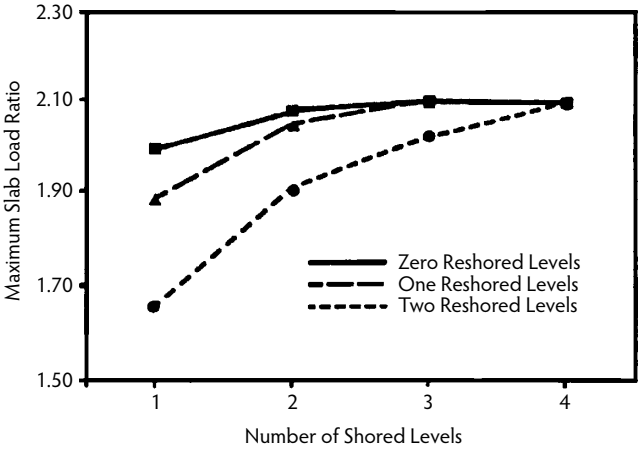

FIGURE 8.22 Influence of the number of shored levels on the maximum slab load. (From Stivaros, P.C. and Halvorsen, G.T., *ACI Struct. J.*, 87(5), 589–596, 1990.)

lower the construction load the floor slabs share. A comparison between the two-shore and five-shore configurations and the simplified method shows that the two-shore configuration is closer to the simplified method. Thus, the simplified method is more suitable for cases with fewer concentrated reaction-type shores per bay. The simplified method underestimates the construction slab loads during the early stages of construction, when a more dense shoring system is used. Figure 8.21 shows how the maximum slab load changes with respect to the number of reshored levels for combinations with one and two levels of shoring. The maximum slab load decreases at a decreasing rate as the number of reshored levels increases.

According to the simplified method, any applied construction load is distributed equally among the interconnected slabs or in proportion to their relative stiffnesses. As the number of slabs in the shoring system increases, the amount of load that each slab shares decreases; however, when compressible shores or reshores are used, the uppermost floor slabs carry most of the applied construction load, leaving the lower slabs without much load to share. This makes the additional reshored levels redundant and ineffective. Figure 8.22 shows the relationship between the number of shored levels, along with various combinations of reshores, and the maximum slab load. The figure shows that as the number of the shored levels increases, the maximum slab load also increases. Although this is true, the maximum slab load occurs on an older slab, which has more strength, when more shored levels are used. During the design of the shoring system, it is important to determine the minimum number of shored levels required so the maximum applied load will occur on a slab that is old enough to have developed the necessary strength to withstand this load. Either the number of shored levels or the construction rate can be controlled. It is also interesting to observe from Figure 8.22 that all reshore combinations, from zero to three reshored levels, tend to converge as the number of shored levels increases; therefore, it is important to determine the maximum number of reshored levels that can cause an appreciable change in the maximum applied construction loads.

8.3 Properties of Concrete at Early Ages

As discussed in detail in Section 8.2, when the usual shore/reshore method of construction is used for multistory buildings, high early-age, short-duration loads are imposed on the slabs. These loads can be comparable in magnitude to, or even exceed, the design service loads. Also, they are applied to concrete slabs that have not achieved their specified concrete strength. The consequences may very well be structural failure, unless adequate precautions are taken during construction, based on proper evaluation of the construction loads and sound knowledge of the early-age properties of concrete. Structural failures

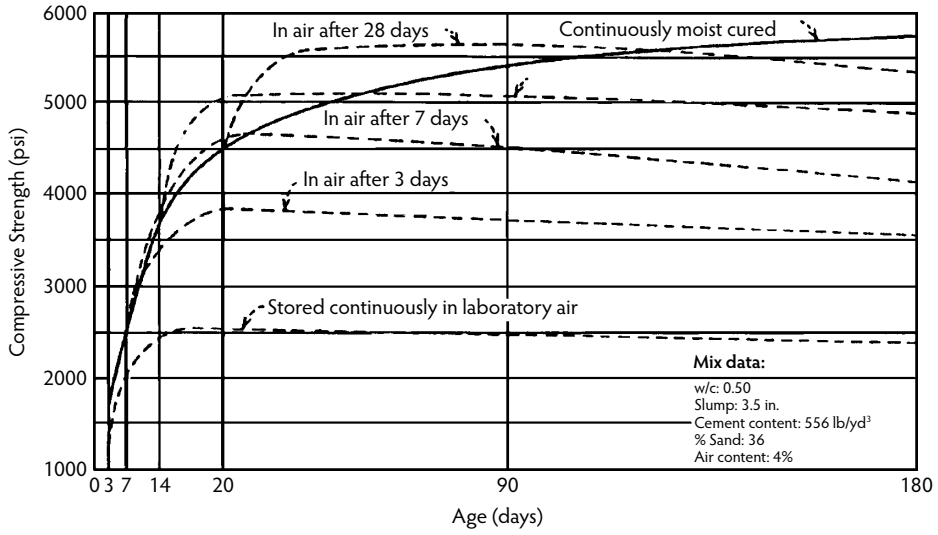

FIGURE 8.23 Compressive strength of concrete dried in laboratory air after preliminary moist curing. (From Price, W.H., *ACI J.*, 22(6), 417–432, 1951.)

may be associated with collapse of a structure or part of a structure or structural member, or they may be associated with structural distress that causes a significant reduction in the capability of a structure to function in the way originally intended. The former may be classed as *strength* failures, while the latter may be referred to as *serviceability* failures. Strength failures occur relatively infrequently but can be catastrophic, sometimes leading to loss of life. Serviceability failures occur more frequently and, although not usually catastrophic or life threatening, may result in significant financial losses. Objectionable cracking or excessive floor-slab deflections are examples of serviceability failure.

Heavy construction loads applied to slabs at early ages may be a major contributing factor to strength failures as well as serviceability failures. To understand the strength-related consequences, which may be due to deficiencies of flexural-axial loading strength, shear strength, or bond strength, a knowledge of the compressive strength, tensile strength, shear strength, and bond strength of concrete is necessary. For an understanding of the serviceability related consequences, a knowledge of the modulus of elasticity, shrinkage, and creep of concrete at early ages is essential.

8.3.1 Compressive Strength

Price (1951) and Klieger (1958) generated considerable information on the development of the compressive strength of concrete under varying temperature and moisture conditions. Temperature and moisture have pronounced effects on the strength development of concrete. Figure 8.23 (Price, 1951) shows that the development of strength stops at an early age when a concrete specimen is exposed to dry air with no previous moist curing. Concrete exposed to dry air from the time it is placed is about 42% as strong at 6 months as concrete that was continuously moist cured. Specimens cured in water at 70°F were found to be stronger at 28 days than those cured in a fog room at 100% relative humidity. The richer mixes showed up to better advantage than the leaner ones under water curing. The strength of the water-cured specimens was about 10% higher than that of the fog-cured specimens for concrete having water/cement ratios of 0.55 by weight.

Curing temperatures have a marked effect on the strength development of concrete. Test results were obtained by casting and curing concrete specimens at different temperatures, and under such treatment the highest temperatures developed the highest 28-day strength. Other concrete specimens were cured at 70°F after holding the specimens at different casting temperatures for 2 hours. Such treatment produced

opposite results, as the specimens made at the lower temperatures produced the highest 28-day strength. It was speculated that concrete cast at high temperatures is weakened by rapid setting, which is not overcome by subsequent curing at 70°F. Continued curing at higher temperatures for the full 28-day period, as was done for some of the first sets of specimens, accelerated the strength development sufficiently to produce the highest strength for the highest temperature. At later ages, however, the specimens made and cured at higher temperatures had lower strengths than those made and cured at lower temperatures.

In Klieger's (1958) investigation, concretes were mixed and placed at temperatures of 40, 55, 73, 90, 105, and 120°F. Specimens were tested at ages 1, 3, 7, and 28 days; 3 months; and 1 year. ASTM Type I, II, and III cements were used. Concretes were made both with and without calcium chloride as an accelerator. An air-entraining agent was added at the mixer to entrain a prescribed amount of air in all of the concretes. In Part I (73°F and lower), all specimens were continuously moist cured (100% relative humidity) at the mixing and placing temperature for 28 days or less, depending on the test age. After the initial 28-day period, half of the remaining specimens for tests at 3 months and 1 year, were stored at 73°F and 100% relative humidity and the other half at 73°F and 50% relative humidity. Additional concretes were mixed and placed at 40°F, and, immediately after placing, the specimens in their molds were stored at 25°F. All surfaces were kept continuously moist (prior to and following removal from the molds at 1 day of age) for 28 days or less, depending on test age. After 28 days, specimens kept for tests at 3 months and 1 year were treated like those stored at other temperatures.

In Part II (73°F and higher), half of the specimens were moist cured for 7 days at the fabrication temperature, and the remainder of the specimens were moist cured for 28 days at the fabrication temperature. At the end of the 7- and 28-day preliminary curing periods, each half was divided into two groups, one cured at 73°F and 100% relative humidity and the other at 73°F and 50% relative humidity. For concretes mixed at 40 and 73°F, the net water/cement ratio was held at the value determined to produce the target slump at 55°F. In Part II, the net water/cement ratio for each concrete was such as to produce a certain target slump at a concrete temperature of 90°F. Continuity between Parts I and II was provided by a repetition of the tests for all the concretes at 73°F; a small difference in net water/cement ratio between the concretes in Parts I and II was found.

Two 6 × 6 × 30-in. beam specimens were cast for each test age and curing condition. Beams were tested in flexure with load applied at the third points of an 18-in. span. Two flexural breaks were obtained for each beam. The two beam ends were tested for compression as 6-in. modified cubes. (For the particular aggregate, the ratio of 6 × 12-in. cylinder strength to 6-in. modified cube strength was taken as 0.93.) For each test age, concrete mix, and curing procedure, two beams were tested, yielding four flexural and four compressive test results for averaging. All strength tests were made at a concrete temperature of 73°F. Specimens stored at temperatures other than 73°F were placed in the 73°F moist room for temperature conditioning 1/2 hour before testing.

Figure 8.24 shows all the compressive strength data for three types of cement with and without accelerator, expressed as percentages of the strengths developed at 73°F for each test age. This figure shows the accelerating effect of temperatures above 73°F on the early-age strengths, with a sacrifice, however, in strength at later ages. On the other hand, concretes placed and cured at temperatures below 73°F, while showing lower strengths at the early ages, show strengths at the later ages in excess of those developed at 73°F. This was true even for concretes mixed and cast at 40°F and stored immediately after casting at 25°F for the first 28 days. For concretes cured initially at low temperatures followed by curing at 73°F, 1-year strengths close to or exceeding those for the concretes cured continuously moist at 73°F were attained only when moist curing was employed. Air drying during this subsequent 73°F period generally resulted in lower strengths, particularly for concretes made with Type I and Type II cements.

The data in Figure 8.24 are for concretes moist cured the first 28 days. In Part II, a 7-day moist-curing period at the fabrication temperature was included for comparison with the 28-day moist-curing period at the fabrication temperature. The qualitative interpretation of results for this 7-day group was similar to that for the 28-day group. The following conclusions were drawn by Klieger (1958):

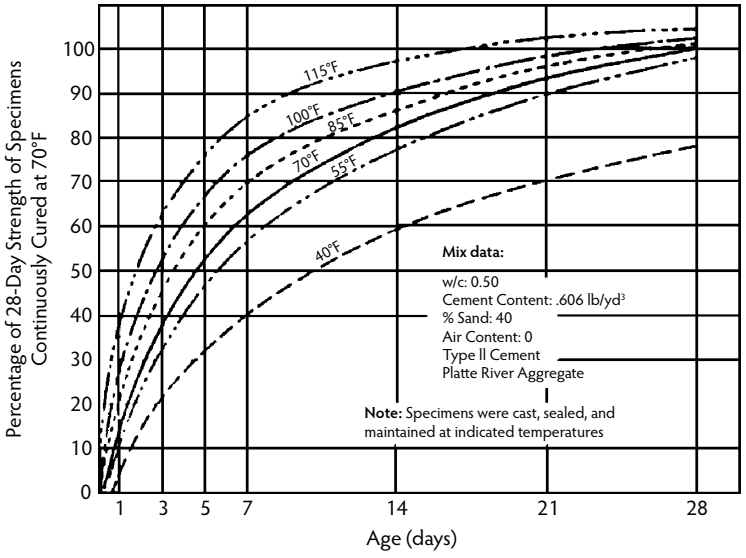

FIGURE 8.24 Effect of temperature on compressive strength of concretes made with different types of cement with and without an accelerator. (From Klieger, P., *ACI J.*, 29(12), 1063–1081, 1958.)

1. At 1, 3, and 7 days, concrete compressive strengths increase with an increase in the initial and curing temperatures of the concrete.
2. Increasing the initial and curing temperatures results in considerably lower compressive strengths at 3 months and 1 year.
3. Compressive strengths of concretes made with the three cement types used were influenced in a like manner by temperature; differences were in degree only.
4. These tests indicated that there is a temperature during the early life of concrete that may be considered optimum with regard to strength at later ages or, more strictly, at comparable degrees of hydration. This temperature is influenced somewhat by cement type. For Types I and II, this temperature appears to be 55°F; for Type III, 40°F.
5. For concretes with calcium chloride added, compressive strength increases due to the accelerator were proportionately greater at early ages and lower temperatures.

ACI Committee 209 (1971) has recommended the following expression for the time-dependent strength of moist-cured (as distinct from steam-cured) concrete using Type I cement:

$$f'_{ct} = \frac{t}{4.00 + 0.85t} f'_c \tag{8.1}$$

where t is the time in days from casting up to loading and f'_c is the 28-day compressive strength of concrete.

The validity of Equation 8.1 at very early ages needs to be examined in view of the data reported above and a significant volume of European data that is also available (Byfors, 1980; RILEM Commission 42-CEA, 1981).

8.3.2 Tensile Strength and Bond Strength

Price (1951) reported data (Table 8.6) from tests at the Portland Cement Association showing relationships among the compressive strength, the tensile strength, and the flexural strength (modulus of rupture) of concrete. It was not stated, but may probably be assumed, that the tensile strength reported was the splitting tensile strength: "The ratio of tensile to compressive strength decreases as the compressive strength increases and approaches a constant of about 7% for higher compressive strength. Other published data

TABLE 8.6 Comparison of Compressive, Flexural and Tensile Strength of Plain Concrete

Strength of Plain Concrete (psi)			Ratio (%)		
Compressive	Modulus of Rupture	Tensile	Modulus of Rupture to Compressive Strength	Tensile Strength to Compressive Strength	Tensile Strength to Modulus of Rupture
1000	230	110	23.0	11.0	48
2000	375	200	18.8	10.0	53
3000	485	275	16.2	9.2	57
4000	580	340	14.5	8.5	59
5000	675	400	13.5	8.0	59
6000	765	460	12.8	7.7	60
7000	855	520	12.2	7.4	61
8000	930	580	11.6	7.2	62
9000	1010	630	11.2	7.0	63

Source: Price, W.H., *ACI J. Proc.*, 22(6), 417–432, 1951.

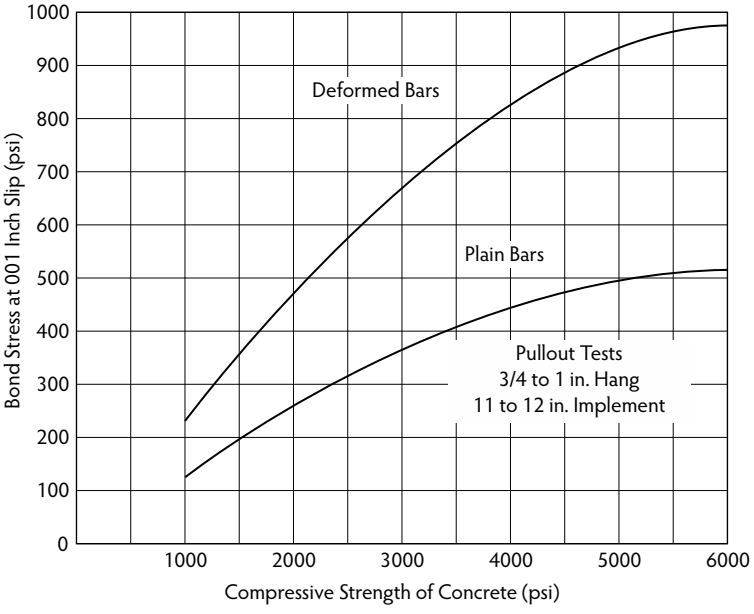

FIGURE 8.25 Variation of bond with strength of concrete. (From Price, W.H., *ACI J.*, 22(6), 417–432, 1951.)

indicate that the ratio of tensile to compressive strength decreases as the age of concrete increases to the same constant value of 7%" (Price, 1951). Figure 8.25 shows in a qualitative way the relationship between bond strength and compressive strength of concrete for plain and deformed bars. The ratio of bond strength to compressive strength decreases as compressive strength increases. The bond strength of the deformed bars is 24% of the compressive strength for 2000-psi concrete and 18% of the compressive strength for 5000-psi concrete. "The relationship of bond to compressive strength apparently is not changed materially by air entrained in the proportions recommended" (Price, 1951).

Klieger's (1958) flexural strength data for the same concretes as were tested for Figure 8.24 showed that the discussion about compressive strength data in the previous section applies equally to the flexural strength data. Flexural strengths at early ages increased with increase in temperature. At later ages, the effect of temperature was reversed. Concretes made and cured at lower temperatures showed the highest flexural strengths at 1 year. The optimum temperatures for flexural strength development appeared to be the same as those for compressive strength. The use of calcium chloride frequently resulted in flexural

strengths at later ages that were somewhat lower than for comparable concretes without calcium chlorides. Maximum reductions noted were on the order of 10%.

In a significant investigation by Gardner and Poon (1976), six series of specimens were cast: three using Type I and three using Type III cement concretes. The specimens for each series were cast from a single batch of ready-mixed concrete. Two series of tests, one made with Type I cement concrete and one with Type III cement concrete, were carried out with the concrete continuously moist cured at 72°F (22°C). Two series of specimens, one made using Type I cement concrete and one with Type III cement concrete, were subjected to extended curing under wet burlap at a steady temperature of 55°F (13°C). The remaining two series were subjected to extended curing under wet burlap at a steady temperature of 35°F (2°C). All specimens were cast at 72°F (22°C). To examine the effect of time on the concrete, specimens were cured at 72°F (22°C) for different periods before exposing them to low temperatures. One third of the specimens of each series were cured for 1 day, one third were cured for 3 days, and the remainder were cured for 7 days at 72°F (22°C) before being transferred to the cooler environment.

Each series involved the casting of 160 standard 6 × 12-in. (150 × 300-mm) cylinders and 80 bond specimens. Five specimens were tested for compressive strength, 5 for tensile strength, and 5 for bond strength at 1, 3, 7, 14, and 28 days and at 3 months for each of the 14 curing schedules. All concretes had a specified cylinder strength of 4000 psi (28 MPa) and a water/cement ratio of approximately 0.5. Compressive and tensile strengths were determined by the standard compressive strength test and the split-cylinder test, respectively, on 6 × 12-in. (150 × 300-mm) cylinders. Bond specimens were made by casting a #6 reinforcing bar into a 6 × 6-in. (150 × 150-mm) cylindrical block of concrete to closely approximate the ASTM standard specimen, which is a 6-in. (150-mm) concrete cube or a 6 × 6 × 12-in. (150 × 150 × 300-mm) block of concrete. Concrete strengths are plotted against the log of time in Figure 8.26 for concretes made with Type I cement and subjected to extended curing at 35°F (2°C). Figure 8.26 was typical of all six batches of concrete. The following conclusions were drawn:

1. Temperature influences the tensile and bond strength development of concrete in much the same manner as it does compressive strength development. Compressive strength, tensile strength, and bond strength are all related, and an increase in one is reflected in the others.
2. The compressive strength, tensile strength, and bond strength of concrete at early ages increases with increased curing temperature. The lower the initial curing temperature the greater the eventual ultimate strength of the concrete, provided curing is continuous.
3. Bond strength and tensile strength are proportional to the 0.8 power of the cylinder strength at the appropriate age. Neither extended curing at temperatures of 35°F (2°C) and 55°F (13°C) nor type of cement appears to have any significant effect on the interrelationship of bond strength or tensile strength and cylinder strength.
4. With respect to construction schedules, there is a 5 to 9% gain in the 7-day and in the 14-day strengths due to casting and curing Type I cement concretes for 3 days and 7 days, respectively, at 72°F (22°C), compared to casting and curing for 1 day at 72°F (22°C).
5. Type III cement concretes exhibited a small strength gain due to prolonged initial curing at 72°F (22°C) when subjected to extended curing at 35°F (2°C) but no strength gain for prolonged initial curing at 72°F (22°C) when subjected to extended curing at 55°F (13°C).

Lew and Reichard (1978) performed three types of tests:

1. Compressive strength tests of cylindrical specimens
2. Splitting tensile tests of cylindrical specimens
3. Bond-strength tests using cylindrical pullout specimens

All three types of tests were made on specimens cured at different temperatures—35°F (2°C), 55°F (13°C), and 73°F (22°C)—and tested at nine ages (1, 2, 3, 5, 7, 14, 21, 28, and 42 days).

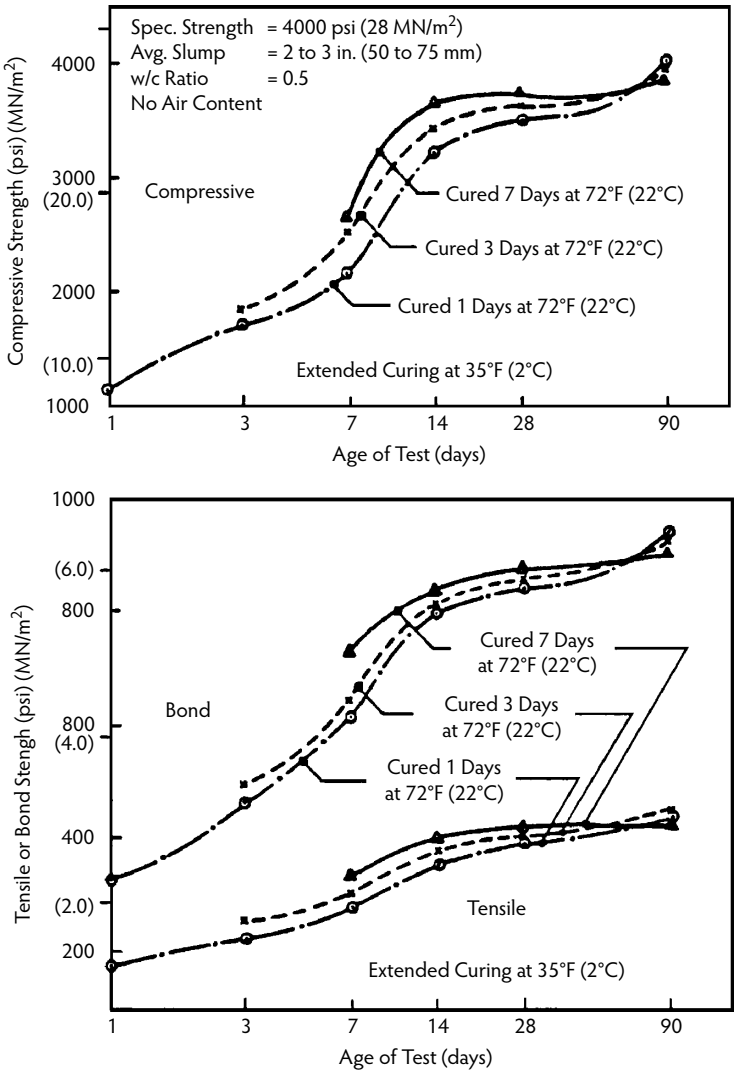

FIGURE 8.26 Variation of concrete strength with temperature for Type I cement concrete cured at 35°F (2°C). (From Gardner, N.J. and Poon, S.M., *ACI J.*, 73(7), 405–409, 1976.)

The combined effect of temperature and time, or *maturity*, usually expressed in degree-days (or hours), may be defined as the sum of the product of the increment of age of cure and the difference between curing and some temperature below which no strength gain takes place. The definition can be written as:

$$M = \sum (T - T_0)\Delta t \tag{8.2}$$

where T is temperature of the concrete at any time, T_0 is a datum temperature below which no strength gain of concrete takes place, and Δt is the increment of time. Taking T_0 = 10°F (–12°C) on the basis of prior tests, Equation 8.2 can be rewritten as:

$$M = \sum (T - 10)\Delta t \tag{8.3}$$

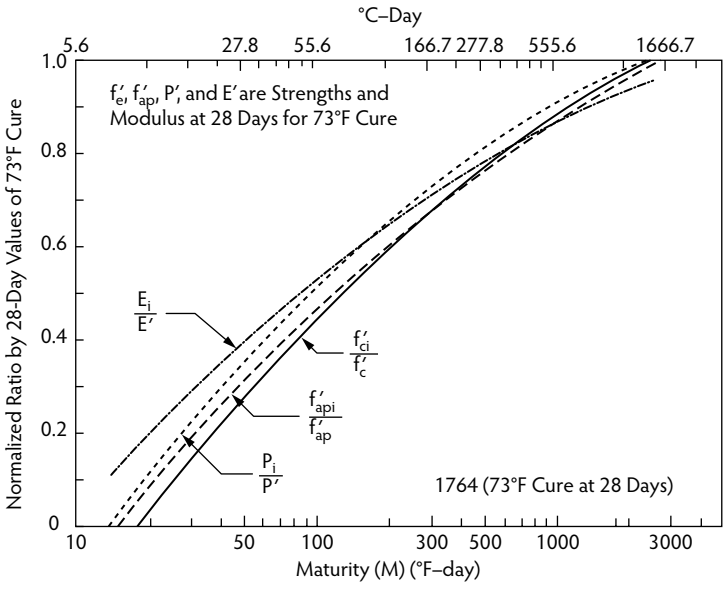

FIGURE 8.27 Mechanical properties normalized with respect to 28-day values vs. maturity. (From Lew, H.S. and Reichard, T.W., *ACI J.*, 75(10), 533–542, 1978.)

where T is in degrees Fahrenheit. Analysis of Lew and Reichard's test data showed that the compressive strength of concrete can be related to maturity expressed in terms of concrete temperature and age of cure. When related to maturity, the elastic modulus data and the splitting tensile strength data of specimens cured at various temperatures could be treated as being from a single group. The pullout strength, when not governed by the yielding of the bar, could be expressed in terms of maturity, thus allowing the specimens cured at various ages to be treated as a single group as well. Figure 8.27 (Lew and Reichard, 1978) shows that, at early ages, the rate of increase in the splitting tensile strength is about the same as that of the compression strength, whereas the rate of increase in the pullout bond strength and the modulus are slightly greater than that of the compressive strength.

Carino and Lew (1982) performed a series of statistical analyses on published data of Gardner and Poon (1976), on published data from the National Bureau of Standards (NBS) (Lew and Reichard, 1978), and on previously unpublished data from the NBS. These data were used to determine the best relationship between the splitting tensile strength and the compressive strength of normal weight concrete, which was then compared with a larger group of published data. The unpublished data were from tests of specimens made with concretes similar to those reported in Lew and Reichard (1978) but which were allowed to cure under ambient, outdoor conditions. Three replicate specimens were tested at ages ranging from 1 to 37 days.

This study clearly indicated that the assumed proportionality of splitting tensile strength to the square root of compressive strength is not the most precise relationship when dealing with a wide range of compressive strengths. The square-root relationship was originally formulated on the basis of tests on mature concrete with strengths generally greater than 2500 psi (17.2 MPa). For low compressive strength, the current ACI formula overestimates splitting tensile strength and underestimates it for high compressive strength. A simple power law of the form $f'_{sp} = (f'_c)^b$ was found to be a more precise representation of data over the full range of concrete strengths. For the Gardner–Poon data and data from the two series of NBS tests mentioned above, the best-fit estimate of b was found to be 0.73. When additional data from four different published references and from other unpublished work at NBS were added to the mix, $f'_{sp} = (f'_c)^{(0.71)}$ seemed to be appropriate for estimating the average expected splitting tensile strength. The function $f'_{sp} = (f'_c)^{(0.71)}$ appeared to give a reasonable lower bound estimate, overestimating about 10% of the data.

8.3.3 Punching Shear Strength

According to Nilson (1991) (who was discussing mature concretes), a reasonable estimate for the split-cylinder strength (f'_{sp}) is 6 to 7 times the square root of f'_c for normal weight concretes. The true tensile strength (f'_t) is on the order of 0.5 to 0.7 times f'_{sp} (3 to 5 $\sqrt{f'_c}$), and the flexural tension strength (f'_r) (modulus of rupture) varies from 1.25 to 1.75 times f'_{sp} (7.5 to 12 $\sqrt{f'_c}$). The smaller of the foregoing factors apply to higher strength concretes and the larger to lower strength concretes. The modulus of rupture controls the behavior of flexural members subject to large bending moments and small shear forces; for large shear forces, the concern becomes safety against premature failure due to diagonal tension in the concrete, resulting from combined shear and longitudinal flexural stresses. In flexural members subject to large shear forces and small bending moments, *web-shear* cracks can be expected to form when the diagonal tension stress in the vicinity of the neutral axis becomes equal to the tension strength of the concrete (3 to 5 $\sqrt{f'_c}$). In members subject to large shear forces as well as large bending moments, *flexure-shear* cracks form when the diagonal tension stress at the tip of one or more flexural cracks exceeds the tensile strength of the concrete.

The information presented on the early-age modulus of rupture and split-cylinder strength of concrete in the previous section is directly relevant to the flexural and diagonal tension failure of beams and one-way slabs; however, as noted, one of the common causes of failure of flat-plate structures during construction is insufficient early-age punching shear strength under relatively high construction loads. Direct knowledge of early-age punching shear strength was thus thought to be desirable and was investigated by Gardner (1960). A relatively large number of circular flat plates were made and subjected to a centrally applied load through a circular steel plate. All steel was located on the tension side of the slabs, and steel ratios ranged from .5 to 5%. Concrete strengths ranged from 2000 to nearly 8000 psi (14 to 56 MPa). Slab thicknesses were 2, 4, and 6 in. (50, 100, and 150 mm). An initial set of experiments was undertaken to determine how punch diameter relates to slab thickness, slab outer diameter, and slab support diameter.

For punching shear failure to occur, at least three slab thicknesses are necessary between the punch and the slab support. Further, the slab outer diameter must be sufficient to enable the slab steel to develop any necessary stress; otherwise, the slab will fail in bond, separating at the reinforcement level. All specimens with zero steel or steel ratios less than .5% failed in flexure. A few conclusions, given below, were drawn.

1. The steel ratio in the region 3 dia from the column should be of the order of 0.5% in each direction, and the spacing should be similar to the effective depth.
2. In all cases, slabs should be detailed so some of the top (negative-moment tension) steel passes through the column.
3. The cube-root relationship between shear strength and concrete strength is preferable to the square-root relationship currently used by ACI Committee 318 (1995).
4. If the punching shear strength is in doubt, the shear perimeter should be increased by using larger columns or column capitals.

8.3.4 Modulus of Elasticity

Figure 8.28 (Byfors, 1980) provides an idea of how the stress–strain relationship of concrete in compression changes with age. The stress and the strain are related to the compressive strength and the corresponding strain, respectively. The arrows in the figure indicate possible unloading. The relationship is practically a straight-line curve at a very early age (5.0 hours). It can be seen that the strain is mainly inelastic. At this early stage, concrete shows properties that are similar to those of a claylike material. A few hours later (7.9 hours), the stress–strain relationship has a completely different character. One can see a clear transition from the elastic to the inelastic part. After 15.8 hours, the curve begins to get the appearance that normally characterizes concrete. The continued changes in the appearance of the stress–strain relationship are not, however, as radical any longer. Expressed in absolute values, the changes are nevertheless large.

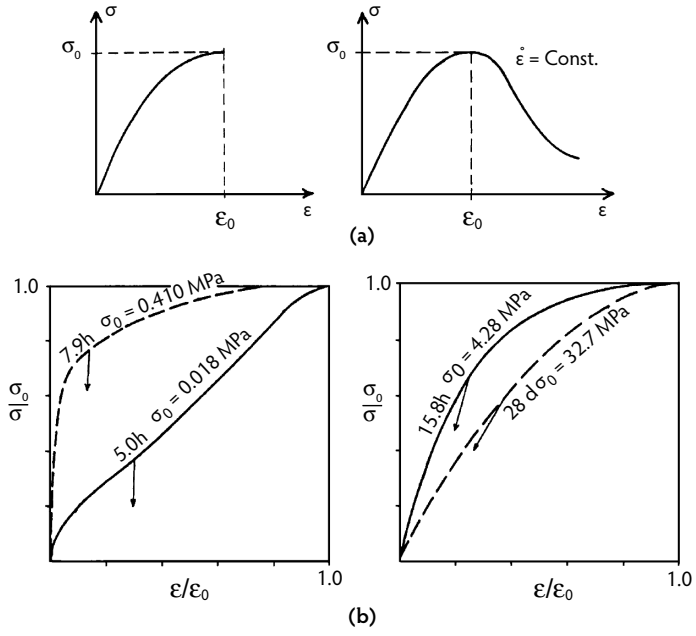

FIGURE 8.28 (a) Basic appearance of the compressive stress–strain relationship under constant stress rate (left) and constant deformation rate (right). (b) Change of shape of compressive stress–strain relationship at early ages. (From Byfors, J., *Plain Concrete at Early Ages*, Fo. 3, No. 80, Swedish Cement and Concrete Research Institute, Stockholm, Sweden, 1980.)

The modulus of elasticity, also referred to as elastic modulus, Young's modulus, and Young's modulus of elasticity, may be defined in general terms as the ratio of normal stress to corresponding strain for tensile or compressive stress below the proportional limit of the material. Few materials, however, conform to Hooke's law throughout the entire range of stress–strain relations; deviations there from are caused by inelastic behavior. If the deviations are significant, the slope of the tangent to the stress–strain curve at the origin, the slope of the tangent to the stress–strain curve at any given stress, the slope of the secant drawn from the origin to any specified point on the stress–strain curve, or the slope of the chord connecting any two specified points on the stress–strain curve may be considered to be the modulus. In such cases, the modulus is designated as the initial tangent modulus, the tangent modulus, the secant modulus, or the chord modulus, respectively, and the stress is stated. Normally, the static modulus of elasticity of concrete is determined as the secant modulus based on short-term experiments but with a certain number of repeated loadings at a low stress level. The stress level for the secant's intersection is normally 30 to 50% of strength. Studies leading to the expression for modulus of elasticity of concrete in ACI Committee 318 are summarized in Pauw (1960), where E_c was defined as the slope of the line drawn from a stress of zero to a compressive stress of $0.45f'_c$.

According to ACI Committee 209 (1971), the effect of age of concrete at the time of loading on the modulus of elasticity of concrete is accounted for when strength of concrete at the time of loading, rather than at 28 days, is inserted into the modulus of elasticity expression given in ACI Committee 318 (1995):

$$E_{ct} = 33w^{1.5}\sqrt{f'_{ct}} \tag{8.4}$$

where E_{ct} is the time-dependent modulus of elasticity of concrete in pounds per square inch, w is the unit weight of concrete in pounds per cubic feet, and f'_{ct} is the time-dependent concrete strength in pounds per square inch.

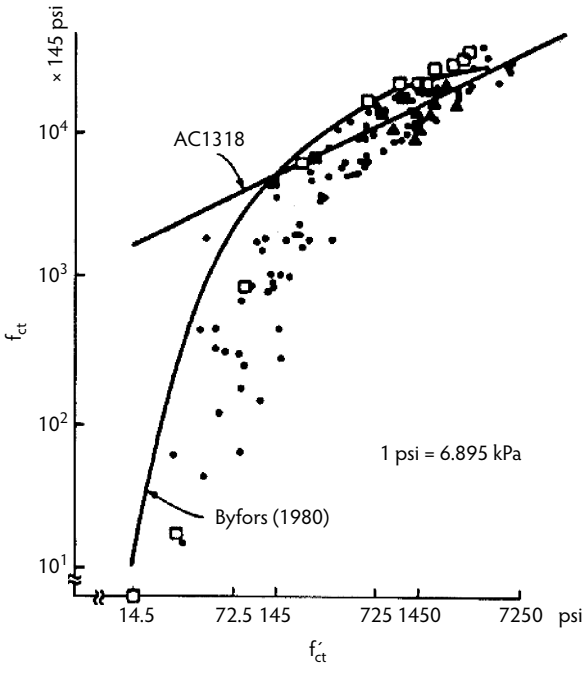

FIGURE 8.29 Modulus of elasticity of concrete at early ages. (From Fintel, M. et al., *Column Shortening in Tall Structures: Prediction and Compensation*, EB108-01D, Portland Cement Association, Skokie, IL, 1987.)

Equation 8.4 for normal weight concrete, when converted to SI units and rounded off, becomes:

$$E_{ct} = 5000\sqrt{f'_{ct}} \tag{8.5}$$

where E_{ct} and f'_{ct} are in megapascals. Figure 8.29 shows a comparison of Equation 8.5 with the experimental information currently available on the modulus of elasticity of concrete at early ages (RILEM Commission 42-CEA, 1981). Concrete strengths of 1 MPa (145 psi) and less are encountered only during the first few hours after concrete is poured and are not of interest here. In the range of practical interest, the ACI equation relating modulus of elasticity and strength agrees quite favorably with the trend of experimental results.

8.3.5 Shrinkage of Unreinforced (Plain) Concrete

Shrinkage of concrete is caused by the evaporation of moisture from the surface. The rate of shrinkage is high at early ages and decreases with an increase in age until the curve becomes asymptotic to the final value of shrinkage. The rate and amount of evaporation and consequently of shrinkage depend greatly upon the relative humidity of the environment, size of the member, and mix proportions of the concrete. In a dry atmosphere, moderate-size members (24-in. or 600-mm diameter) may undergo up to half of their ultimate shrinkage within 2 to 4 months, whereas identical members kept in water may exhibit growth instead of shrinkage. In moderate-size members, the inside relative humidity has been measured at 80% after 4 years of storage in a laboratory at 50% relative humidity.

8.3.5.1 Basic Value of Shrinkage

Let e_s denote the ultimate shrinkage of 6-in. (150-mm)-diameter standard cylinders (volume-to-surface or *v*:*s* ratio = 1.5 in. or 38 mm) moist-cured for 7 days and then exposed to 40% ambient relative humidity. If concrete has been cured for less than 7 days, multiply e_s by a factor linearly varying from

1.2 for 1 days of curing to 1.0 for 7 days of curing (ACI Committee 209, 1971). Attempts have been made in the past to correlate e_s with parameters such as concrete strength. In view of available experimental data (Russell and Corley, 1977), it appears that no such correlation may in fact exist. The only possible correlation is probably that between e_s and the water content of a concrete mix (Troxell et al., 1968). In the absence of specific shrinkage data for concretes to be used in a particular structure, the value of e_s may be taken as between 500×10^{-6} in./in. (mm/mm) (low value) and 800×10^{-6} in./in. (mm/mm) (high value) (Fintel et al., 1987). The latter value has been recommended by the ACI Committee 209 (1971).

8.3.5.2 Effect of Member Size

Because evaporation occurs from the surface of members, the volume-to-surface ratio of a member has a pronounced effect on the amount of its shrinkage. The amount of shrinkage decreases as the size of the specimen increases. For shrinkage of members having volume-to-surface ratios different from 1.5, e_s must be multiplied by the following factor:

$$SH_{v:s} = \frac{0.037(v:s) + 0.944}{0.177(v:s) + 0.734} \tag{8.6a}$$

where *v*:*s* is the volume-to-surface ratio in inches. The metric equivalent of Equation 8.6a is:

$$SH_{v:s} = \frac{0.015(v:s) + 0.944}{0.070(v:s) + 0.734} \tag{8.6b}$$

where *v*:*s* is the volume-to-surface ratio in millimeters. As indicated in Fintel et al. (1987), Equation 8.6 is based on laboratory data (Hansen and Mattock, 1966) and European recommendations (CEB, 1964, 1972). Much of the shrinkage data available in the literature were obtained from tests on prisms of a 3 × 3-in. (75 × 75-mm) section (*v*:*s* = 0.75 in. or 19 mm). According to Equation 8.6, the size coefficient for prisms of that size is 1.12. Thus, shrinkage measured on a prism of a 3 × 3-in. (75 × 75-mm) section must be divided by 1.12 before the size coefficient given by Equation 8.6 is applied. It should be cautioned, however, that as the specimen size becomes smaller, the extrapolation to full-size members becomes less accurate.

8.3.5.3 Effect of Relative Humidity

The rate and amount of shrinkage greatly depend upon the relative humidity of the environment. If ambient relative humidity is substantially greater than 40%, then e_s must be multiplied by:

$$SH_H = \begin{cases} 1.40 - 0.010H & \text{for } 40 \le H \le 80 \\ 3.00 - 0.030H & \text{for } 80 \le H \le 100 \end{cases} \tag{8.7}$$

where H is the relative humidity in percent. Average annual values of H should probably be used. Maps giving average annual relative humidities for locations around the United States are available (Fintel et al., 1987). If locally measured humidity data are available, however, they are likely to be more accurate than information such as that included in Fintel et al. (1987) and should be used in conjunction with Equation 8.7, which is based on ACI Committee 209 (1971) recommendations. A comparison with European recommendations is shown in Fintel et al. (1987). If shrinkage specimens are stored under job-site conditions rather than under standard laboratory conditions, the correction for humidity, as given by Equation 8.7, should be eliminated.

8.3.5.4 Progress of Shrinkage with Time

Hansen and Mattock (1966) established that the size of a member influences not only the final value of shrinkage but also the rate of shrinkage, which appears to be only logical. Their expression giving the progress of shrinkage with time is:

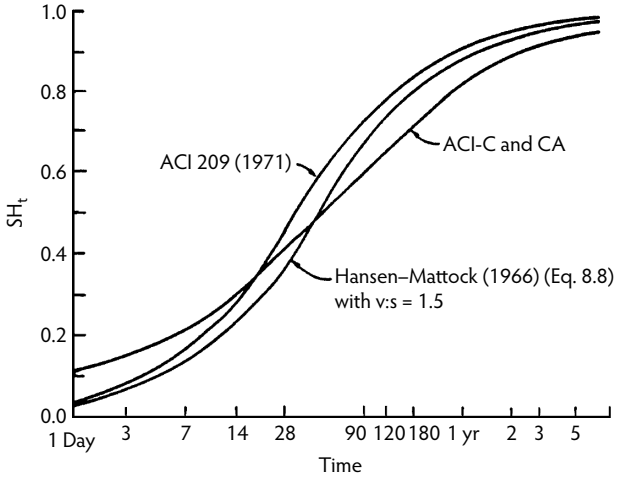

FIGURE 8.30 Progress of shrinkage with time. (From Fintel, M. et al., *Column Shortening in Tall Structures: Prediction and Compensation*, EB108-01D, Portland Cement Association, Skokie, IL, 1987.)

$$SH_t = \frac{\in_{st}}{\in_s} = \frac{t}{26.0e^{0.36(v:s)} + t} \tag{8.8}$$

where $\in_{st}$ and $\in_s$ are shrinkage strains up to time t and time infinity, respectively, and t is measured from the end of moist curing. Equation 8.8 is compared in Figure 8.30 with the progress of shrinkage curve from the *Recommendations for an International Code of Practice for Reinforced Concrete* (CBE, 1964). Also shown in Figure 8.30 is a comparison of Equation 8.8 with the progress of shrinkage relationship recommended by ACI Committee 209 (1971). It should be noted that both the ACI and Cement and Concrete Association (C&CA) (CBE, 1964) and the ACI Committee 209 (1971) relationships are independent of the volume-to-surface ratio.

8.3.6 Creep of Unreinforced (Plain) Concrete

Creep is a time-dependent increment of the strain of a stressed element that continues for many years. The basic phenomenon of creep is not yet conclusively explained. During the initial period following the loading of a structural member, the rate of creep is significant. The rate diminishes as time progresses until it eventually approaches zero. Creep consists of two components:

1. Basic (or true) creep occurs under conditions of hygral equilibrium, which means that no moisture movement occurs to or from the ambient medium. In the laboratory, basic creep can be reproduced by sealing a specimen in copper foil or by keeping it in a fog room.
2. Drying creep results from an exchange of moisture between the stressed member and its environment. Drying creep has its effect only during the initial period under load.

Creep of concrete is very nearly a linear function of stress up to stresses that are about 40% of the ultimate strength. This includes all practical ranges of stresses in columns and walls. Beyond this level, creep becomes a nonlinear function of stress. For structural engineering practice, it is convenient to consider specific creep, which is defined as the ultimate creep strain per unit of sustained stress.

8.3.6.1 Value of Specific Creep

Specific creep values can be obtained by extrapolating results from a number of laboratory tests performed on samples prepared from the actual mix to be used in a structure. It is obvious that sufficient time for such tests must be allowed prior to the start of construction, as reliability of the prediction improves

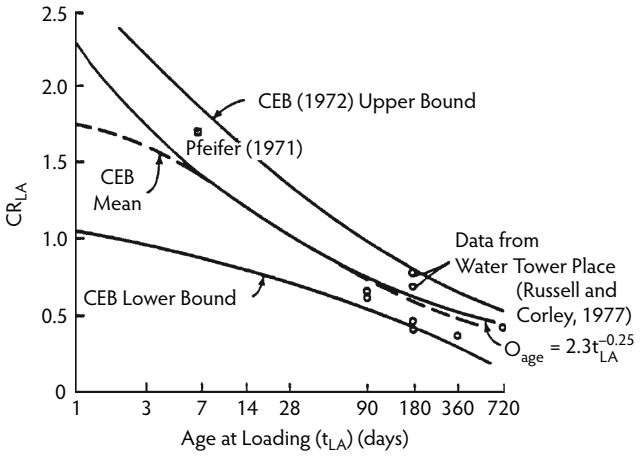

FIGURE 8.31 Creep vs. age of concrete at time of loading. (From Fintel, M. et al., *Column Shortening in Tall Structures: Prediction and Compensation*, EB108-01D, Portland Cement Association, Skokie, IL, 1987.)

with the length of time over which creep is actually measured. A way of predicting basic specific creep (excluding drying creep), without testing, from the modulus of elasticity of concrete at the time of loading was proposed by Hickey (1968) on the basis of long-term creep studies at the Bureau of Reclamation in Denver. A simpler suggestion was made in Fintel et al. (1987), as described below:

Let ε_c denote the specific creep (basic plus drying) of 6-in. (150-mm)-diameter standard cylinders (*v*:*s* = 1.5 in. or 38 mm) exposed to 40% relative humidity following about 7 days of moist curing and loaded at the age of 28 days. In the absence of specific creep data for concretes to be used in a particular structure, the following likely values of ε_c may be used:

$$\in_c = 0.003/f_c' \text{ (low value) to } 0.005/f_c' \text{ (high value)} \tag{8.9a}$$

where $\in_c$ is in inch per inch per kips per square inch if f_c' is in kips per square inch, or in inch per inch per pounds per square inch if f_c' is in pounds per square inch. The metric equivalent of Equation 8.9a is:

$$\in_c = 0.000435/f_c' \text{ (low value) to } 0.000725/f_c' \text{ (high value)} \tag{8.9b}$$

where $\in_c$ is in millimeter per millimeter per megapascal if f_c' is in megapascal, or in millimeter per millimeter per kilopascal if f_c' is in kilopascal. The lower end of the proposed range is in accord with specific creep values suggested by Neville (1981). The upper end agrees with laboratory data obtained by testing the concretes used in Water Tower Place in Chicago (Russell and Corley, 1977).

8.3.6.2 Effect of Age of Concrete at Loading

For a given mix of concrete, the amount of creep depends not only on the stress level but also to a great extent on the age of the concrete at the time of loading. Figure 8.31 shows the relationship between creep and age at loading as developed by Comité Européen du Béton (CEB, 1972), using available information from many tests. The coefficient CR_{LA} relates the creep for any age at loading to the creep of a specimen loaded at the age of 28 days. The 28-day creep is used as a basis of comparison, the corresponding CR_{LA} being equal to 1.0. Figure 8.31 also depicts the following suggested relationship (Fintel et al., 1987) between creep and age at loading:

$$CR_{LA} = 2.3t_{LA}^{-0.25} \tag{8.10}$$

where t_{LA} is the age of concrete at the time of loading, in days. The form of Equation 8.10 is as suggested by the ACI Committee 209 (1971). Equation 8.10 gives better correlation with the CEB mean curve than the corresponding equation suggested by the ACI Committee 209. Figure 8.31 also provides comparison with a few experimental results (Lew and Reichard, 1978; Pfeifer et al., 1971). According to Equation 8.10, the creep of concrete loaded at 7 days of age is 41% higher than that of concrete loaded at 28 days.

8.3.6.3 Effect of Member Size

Creep is less sensitive to member size than shrinkage, as only the drying-creep component of the total creep is affected by the size and shape of members, whereas basic creep is independent of size and shape. For members with volume-to-surface ratios different from 1.5 in. or 38 mm, $\in_c$ should be multiplied by:

$$CR_{v:s} = \frac{0.044(v:s)+0.934}{0.1(v:s)+0.85} \tag{8.11a}$$

where *v*:*s* is the volume-to-surface ratio in inches. The metric equivalent of Equation 8.11a is:

$$CR_{v:s} = \frac{0.017(v:s)+0.934}{0.039(v:s)+0.85} \tag{8.11b}$$

where *v*:*s* is the volume-to-surface ratio in millimeters. As indicated in Fintel et al. (1987), Equation 8.11 is based on laboratory data (Hansen and Mattock, 1966) and European recommendations (CEB, 1964, 1972). Much of the creep data available in the literature were obtained by testing 6-in. (150-mm)-diameter standard cylinders wrapped in foil. The wrapped specimens simulated very large columns. Equation 8.11 yields a value of $CR_{v:s}$ equal to 0.49 for *v*:*s* = 100. Thus, it is suggested that creep data obtained from sealed specimen tests should be multiplied by $2(1/0.49 \cong 2)$ before the modification factor given by Equation 8.11 is applied to such data.

8.3.6.4 Effect of Relative Humidity

For an ambient relative humidity greater than 40%, ε_c should be multiplied by the following factor, as suggested by ACI Committee 209 (1971):

$$CR_H = 1.40 - 0.01H \tag{8.12}$$

where H is the relative humidity in percent. Again, it is suggested that the average annual value of H be used.

8.3.6.5 Progress of Creep with Time

The progress of creep relationship recommended by ACI Committee 209 (1971) is given by the following expression:

$$CR_t = \frac{\in_{ct}}{\in_c} = \frac{t^{0.6}}{10+t^{0.6}} \tag{8.13}$$

where $\in_{ct}$ is the creep strain per unit stress up to time t, and t is measured from the time of loading. This relationship is plotted in Figure 8.32, where it compares well with the creep-vs.-time curve suggested in European recommendations (CEB, 1964).

8.3.6.6 Irreversible Nature of Creep

Another important aspect of creep of concrete must be addressed. Figure 8.33 shows the strain history of a concrete specimen that was stored in air at near 100% relative humidity to eliminate shrinkage and subjected to a sustained axial stress that was removed at 120 days from the time of loading. The instantaneous recovery is followed by a gradual decrease in strain, called *creep recovery*. The shape of the creep-

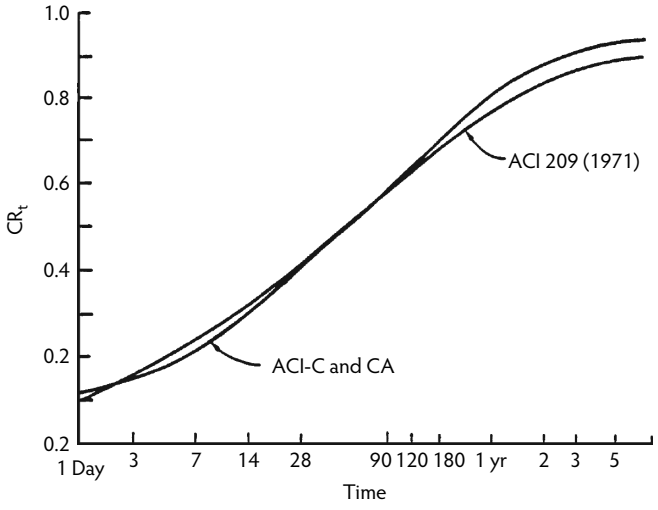

FIGURE 8.32 Progress of creep with time. (From Fintel, M. et al., *Column Shortening in Tall Structures: Prediction and Compensation*, EB108-01D, Portland Cement Association, Skokie, IL, 1987.)

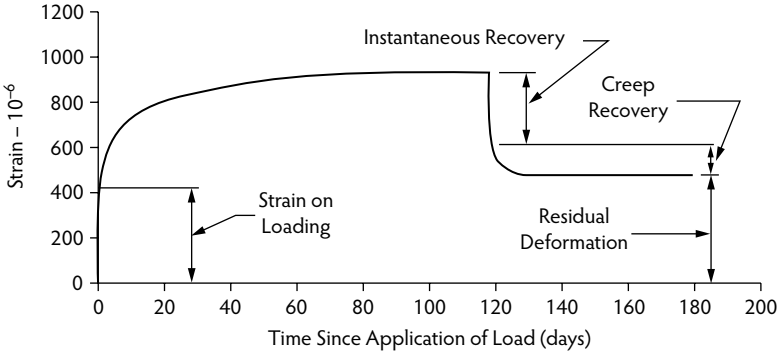

FIGURE 8.33 Creep strain vs. time when part of sustained load is removed at a certain time after application. (From Fintel, M. et al., *Column Shortening in Tall Structures: Prediction and Compensation*, EB108-01D, Portland Cement Association, Skokie, IL, 1987.)

recovery curve is similar to that of the creep curve, but the recovery approaches its maximum value much more rapidly. The reversal of creep is not complete, so any sustained application of load, even over only a day, results in a residual deformation (Neville, 1981).

8.3.7 Effects of Drying on Flexural Cracking

Hover (1988) pointed out that the resistance to flexural cracking in beams and slabs decreases sharply during periods in which the surface of the concrete is drying, such as the period that immediately follows the removal of forms. Hover considered a 6-in. (150-mm)-thick reinforced concrete slab with a concrete compression strength of 4000 psi (28 MPa). The solid lines in Figure 8.34a show the increase in the allowable superimposed live load as a function of the amount of reinforcing steel for continuous spans of 14 to 18 ft (4.2 to 5.4 m). The allowable load was determined by subtracting the factored dead load from the ultimate load and dividing the result by an appropriate load factor. The dotted lines in Figure 8.34a indicate the superimposed live load that caused cracking of the same slabs. Note that, for lightly reinforced slabs, the cracking load is actually greater than the safe allowable load. This means that cracking will be avoided by complying with the load limitations imposed on the basis of strength calculations. Whereas the allowable

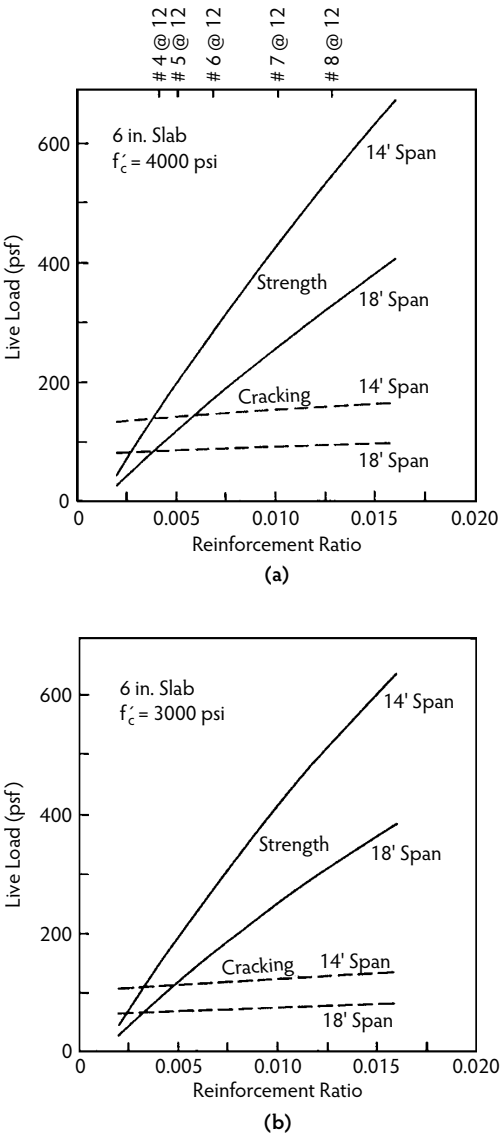

FIGURE 8.34 Allowable live load calculated on the basis of strength vs. cracking live load: (a) f_c' = 4000 psi (28 MPa); (b) f_c' =3000 psi (21 MPa). (From Hover, K.C., in *Forming Economical Concrete Buildings: Proceedings of the Third International Conference*, SP107, American Concrete Institute, Farmington Hills, MI, 1988, pp. 169–184.)

load on the basis of strength considerations increases dramatically with an increasing amount of reinforcing steel, the cracking load increases by only 25% or so for an 8-fold increase in the amount of reinforcing steel. For members with the maximum allowable amount of reinforcing steel, the safe load on the basis of strength exceeds the cracking load by a factor of four. One would therefore expect heavily reinforced slabs and beams to crack at loads well below the safe or allowable load calculated on the basis of strength.

In Figure 8.34b, it is assumed that the same slabs have a compressive strength of only 3000 psi (21 MPa) at the time of load application. Note that this case corresponds to the above 4000-psi (28-MPa) concrete about 7 days after casting, when the concrete has attained approximately 75% of its expected 28-day strength. Comparison of Figure 8.34a with Figure 8.34b shows an approximate 6% decrease in the allowable load on the basis of strength and an approximate 20% decrease in the cracking load for a compression strength decrease from 4000 psi to 3000 psi (28 MPa to 21 MPa). Thus, low concrete

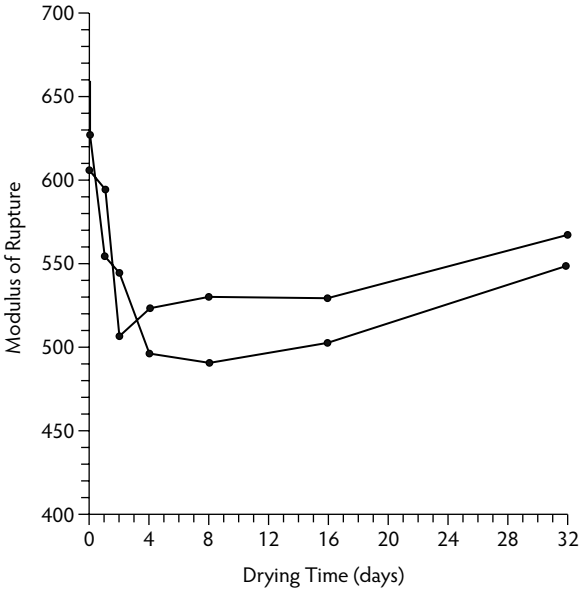

FIGURE 8.35 Data presented by Walker and Bloem (1957b) concerning the influence of drying on the flexural strength of concrete. (From Hover, K.C., in *Forming Economical Concrete Buildings: Proceedings of the Third International Conference*, SP107, American Concrete Institute, Farmington Hills, MI, 1988, pp. 169–184.)

compressive strength has a more significant effect on resistance to cracking than on the strength of the slabs considered in these examples.

Calculation of the cracking load in the above example was done using $f_r = 7.5\sqrt{f_c'}$ as in ACI Committee 318 (2005). Walker and Bloem (1957a,b) and Hover (1984) studied the influence of surface drying on flexural tension strength. The essential results are shown in Figure 8.35, in which the modulus of rupture (MOR) is shown as a function of the time during which the concrete test specimen is exposed to air drying. The modulus of rupture of wet concrete is seen to decrease immediately upon exposure to air. This decrease continues for several days of air drying until a minimum is reached after 3 to 6 days, followed by a slow restoration of the original wet MOR. Continued slow drying eventually leads to a modulus of rupture that is greater than the original wet-tested value. It was found that the MOR could vary from a high of $16\sqrt{f_c'}$ to an apparent lower limit of approximately $4\sqrt{f_c'}$, depending entirely on moisture conditions at the time of testing. Critically, during the first few days and hours of surface drying, the actual modulus of rupture (and therefore the actual cracking resistance) could be as little as 55% of the commonly expected value ($4\sqrt{f_c'}$ rather than $7.5\sqrt{f_c'}$).

The surface of concrete beams and slabs begins to dry immediately upon the removal of the formwork and the subsequent exposure to dry, moving air. While this surface drying is taking place, the removal of shoring and further construction operations load the members. The removal of forms and shores from flexural members is therefore a delicate issue, not only because of the strength development of early-age concrete but also because the surface drying, which is an almost unavoidable consequence of form removal, can decrease the cracking resistance by almost 50%.

To further investigate the phenomenon, beam specimens were cast in forms with steel sides and oiled plywood bottoms. Four days after casting, the forms were removed from three beams, which were then permitted to dry for 4 hours in laboratory air. Three other beams were removed from their forms one at a time and immediately tested so as to avoid appreciable air drying. The average MOR of the beams that were tested immediately upon form removal was 573 psi (4.0 MPa), and the average MOR of the beams that had dried for 4 hours was 450 psi (3.1 MPa), representing a 25% decrease in cracking resistance due to short-term drying.

It is not unreasonable to envision a situation in which the conditions of this experiment are realized on the jobsite, where the removal of beam sides may precede the removal of the beam bottom and supporting shoring by several hours. In that case, the self-weight of the slab or beam would be applied during this critical drying period. Similarly, in the case of rapid construction where the weight of falsework, materials, flying forms, etc. is applied to the top of a recently stripped beam or slab, it is likely that superimposed load would be applied during the critical drying period during which the cracking resistance is substantially reduced.

As part of a related experiment, flexural specimens were cast against steel forms with oiled plywood bottoms, with companion specimens cast in similar forms that had been lined with polyethylene. From tests conducted at 4 hours, 2 hours, and immediately after removal of forms, the modulus of rupture of the beams with the plastic-lined forms was on an average 25% greater than for the beams cast in steel and wood forms. When companion specimens were tested after 28 days of drying in laboratory air, the results for the two types of forms were statistically indistinguishable. It was concluded that the influence of the form surface on the cracking resistance was primarily due to the effects of moisture conditions at early ages. It was pointed out that timing the removal of forms and shores so as not to load a member while the concrete surface is drying can reduce the incidence of flexural cracking or can increase the applied load necessary to initiate such cracking. The use of smooth form surfaces or nonabsorptive form liners may be beneficial in reducing flexural cracking.

8.4 Strength Consequences of Construction Loads

It would be instructive to begin this section with the following four paragraph reproduced, with only minor paraphrasing, from Kaminetzky and Stivaros (1994):

> Throughout the history of concrete construction, numerous construction failures have occurred. Many statistical surveys point out that failures and total collapses occur more frequently during construction than during the service life of a structure. Also, it has been well documented that failure of concrete structures during construction most often occur as a result of formwork failure, concrete member failure due to overloading, or lack of concrete strength.
>
> The most common and often devastating failures are punching shear failures. These are triggered by a localized failure around a single column at an upper-level floor, resulting in progressive collapse going all the way down to the lowest level. Such a domino-effect failure can be stopped by localizing it to a single level. Because punching shear is the weakest link in the chain, the use of large-size columns coupled with continuous reinforcing bars running through the column periphery at both the top and the bottom of the slab will minimize the possibility of progressive collapse.
>
> The most devastating and well-known collapses, during construction, resulting from punching shear, are those that occurred at Bailey's Crossroads, Virginia (Skyline Plaza) (Leyendecker and Fattal, 1977), Commonwealth Avenue, Boston, Massachusetts (1971); and Cocoa Beach, Florida (Harbour Cay Condominiums) (Lew et al., 1982a,b). All of these multistory flat-plate buildings in late stages of construction collapsed vertically in a progressive manner to the ground. The triggering cause was typical: localized punching shear failure at the slab–column connection. Premature removal of formwork coupled with insufficient concrete strength at the time of the collapse were partially blamed for these disasters. The maturity of concrete was affected by the low temperatures that prevailed during the construction of these projects.
>
> Although the Cocoa Beach collapse was mainly attributed to design and construction errors and not directly to concrete strength, procedures for concrete strength determination prior to the removal of forms were flawed. Construction records showed that laboratory-cured cylinders were used in order to determine the actual field strength of the slabs prior to stripping, where proper procedures and common sense dictated testing of field-cured cylinders.

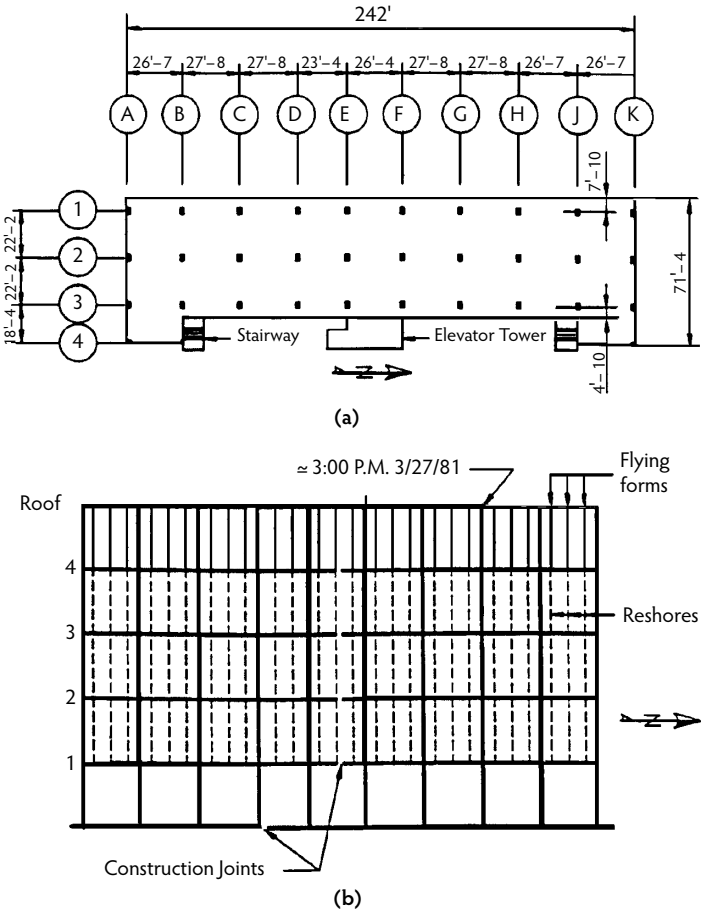

FIGURE 8.36 (a) Typical floor plan of the Harbour Cay Condominium, and (b) assumed state of construction at the time of collapse. (From Stivaros, P.C. and Halvorsen, G.T., *Concrete Int.*, 13(8), 57–62, 1991.)

A reexamination of the Harbour Cay Condominium failure later attributed it more directly to deficiency of punching shear strength (Stivaros and Halvorsen, 1992). The Harbour Cay was a five-story flat-plate concrete building. A typical floor framing plan is shown in Figure 8.36. At the time of collapse, flying forms on the fifth floor supported the fresh concrete roof slab. Three levels of wood reshores rested below. Figure 8.36 shows the flying form and reshore layout and indicates the portion of the roof believed to have been in place at the time of collapse.

National Institute of Standards and Technology (NIST) investigators (Lew et al., 1982a) used the ICES-STRUDL II finite-element program to analyze the Harbour Cay structure. The finite-element model consisted of rectangular plate bending elements for the columns and three-dimensional truss elements for the shoring system. The distribution of loads from the shoring and reshoring procedure was examined by means of the Grundy–Kabaila simplified method. The analysis indicated that, when all the floors were reshored to the ground, the removal of the flying forms at the topmost level completely relieved the forces in the reshores. The existing slabs always supported their own dead load and did not share in supporting a portion of the load of the newly cast floor. Only after the first-story reshores were removed, thus removing a direct load path to the ground, did the existing floor slabs share the load of a newly cast slab. These observations stem from Grundy–Kabaila's basic assumption of an infinitely stiff shoring system.

As a result of the above observations, to determine the state of load distribution at the time of collapse, NIST investigators studied two separate load cases (Figure 8.37). In the first, the structure without reshores

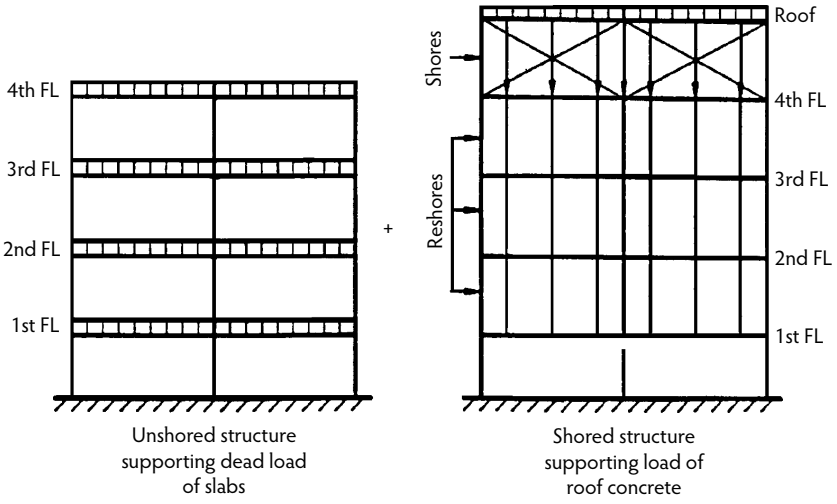

FIGURE 8.37 Two load cases considered in NIST analysis of Harbour Cay Condominium. (From Stivaros, P.C. and Halvorsen, G.T., *Concrete Int.*, 13(8), 57–62, 1991.)

was analyzed under the dead load of the slabs. In the second, the reshored structure was analyzed under the load of the fresh concrete and the formwork. The final result was obtained by superimposing the results of the two analyses. Given in Figure 8.38a are the combined punching shear forces, in kips, for the slab-column connections along column line 2 of the building.

Stivaros and Halvorsen (1992) carried out a preliminary equivalent frame analysis of the Harbour Cay failure, using the same structural data and loading conditions as those used by NIST investigators. The preliminary analysis used the plane frame capabilities of ICES-STRUDL II. The results of this analysis are shown in Figure 8.38a in square brackets. After the preliminary analysis indicated reasonable results, Stivaros and Halvorsen developed their special-purpose computer program [Stivaros and Halvorsen, 1990] that recognized time-dependent material properties and time in the construction process. This program was applied to the construction-load distribution of the Harbour Cay Condominium failure in two different ways. First, the structure was analyzed according to the two loading cases and structural details identified by Lew et al. (1982a). The results of this first analysis are shown in parentheses in Figure 8.38a.

An alternative approach assumed more realistic construction-loading conditions. Grundy–Kabaila's simplified method, as mentioned, assumes an infinitely stiff shoring system; however, the Harbour Cay Condominium used compressible wooden reshores. In the course of the alternative analysis, the program built the structure from the first floor to the roof and considered the effects of all the cycles of loading and unloading as the construction progressed upward. Thus, the effect of compressible reshores could be assessed. Variations in concrete maturity, strength, and stiffness are also incorporated. The punching shear forces at slab-column joints along the height of column stack C-2 are shown in Figure 8.38b. The results of the alternative analysis, which considered the two separate loading cases, are shown in parentheses.

The accuracy of the Grundy–Kabaila simplified method was tested against observations of the Harbour Cay Condominium collapse. Figure 8.38c shows the punching shear forces at every slab–column joint along the height of column stack C-2. The first number indicates the force obtained by the alternative equivalent multi-bay frame, the second number (in parentheses) represents the force obtained by the alternative method using a single-bay model, and the third number (in square brackets) represents the force obtained from the simplified method that invariably uses a single-bay model. A comparison shows that the alternative equivalent single-bay model and the simplified method underestimate the punching shear forces along column stack C-2 on the top floor by 13 and 21%, respectively, as compared to the results of the equivalent multi-bay frame model. On the floors below, both the simplified method and the equivalent single-bay frame model differ by smaller percentages from the equivalent multi-bay frame model.

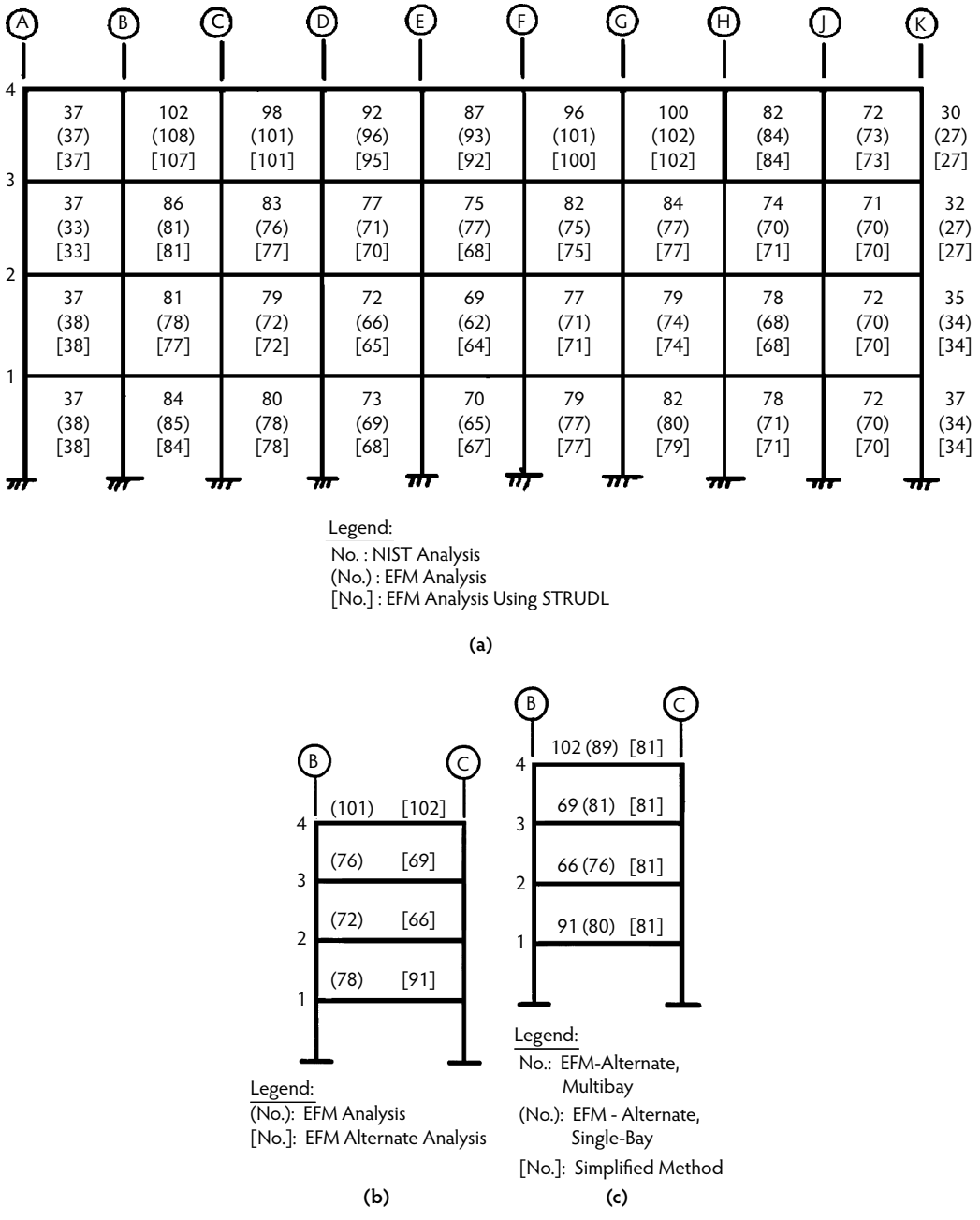

FIGURE 8.38 (a) Punching shear forces along column line 2 (kips); (b) slab loads on bay B-C from multi-bay EFM analysis (kips); (c) slab loads on bay B-C from EFM and simplified method (kips), Harbour Cay Condominium analysis. (From Stivaros, P.C. and Halvorsen, G.T., *Concrete Int.*, 13(8), 57–62, 1991.)

Based on the simplified method and the equivalent single-bay frame analysis, punching shear force at the top slab–column joint along column stack C-2 was within the punching shear strength of that joint; however, analysis based on the equivalent multi-bay frame model indicated that the available punching shear strength was exceeded at the same joint. According to Stivaros and Halvorsen (1992), "Here is exactly where the significance of the EFM multi-bay model lies…."

TABLE 8.7 Development of Tensile/Bond/Shear Strength, Percent of 28-day, 73°F (22.8°C) Value

	Type I Cement Temperature			Type III Cement Temperature		
Aged (day)	73°F (22.8°C)	55°F (12.8°C)	40°F (4.4°C)	73°F (22.8°C)	55°F (12.8°C)	40°F (4.4°C)
1	0.31[a]	0.15[a]	0.03[a]	0.54[a]	0.33[a]	0.11[a]
2	0.47	0.28	0.11	0.65	0.50	0.30
3	0.59[a]	0.40[a]	0.18[a]	0.74[a]	0.62[a]	0.43[a]
4	0.66	0.49	0.24	0.78	0.66	0.54
5	0.72	0.57	0.32	0.81	0.70	0.63
6	0.76	0.63	0.39	0.83	0.73	0.70
7	0.79[a]	0.68[a]	0.44[a]	0.85[a]	0.75[a]	0.77[a]
8	0.81	0.72	0.48	0.86	0.77	0.80
9	0.83	0.75	0.52	0.88	0.79	0.82
10	0.85	0.77	0.56	0.89	0.81	0.84
11	0.86	0.80	0.59	0.90	0.82	0.86
12	0.88	0.82	0.62	0.91	0.84	0.88
13	0.89	0.84	0.64	0.92	0.85	0.89
14	0.90	0.86	0.67	0.92	0.86	0.90
21	0.96	0.94	0.80	0.97	0.93	0.99
28	1.00[a]	1.02[a]	0.88[a]	1.00[a]	0.96[a]	1.07[a]

[a] Klieger's (1958) original data.

Source: Gardner, N.J., *Concrete Int.*, 7(4), 28–34, 1985.

8.4.1 Safety Analysis

Gardner (1985) was the first to attempt a systematic safety analysis of construction (shoring/reshoring) schemes for multistory buildings, as described in this section. The strength of a reinforced concrete slab is a function of the design (factored) load, age of the slab, and the critical mode of behavior of the slab: flexure, bond, or shear. The required strength for various live-load/dead-load ratios, in terms of dead load, can be calculated from ACI 318-05 (ACI Committee 318, 2005) Appendix C as follows:

$$U = 1.4D + 1.7L = D\left[1.4 + 1.7\frac{L}{D}\right] \tag{8.14}$$

Design strength (nominal strength reduced by the appropriate strength-reduction factor) must equal or exceed the required strength and was assumed by Gardner to equal the required strength. It should be noted that, in U.S. design practice, the design strength is assumed to be available at 28 days of age. The strength available at the early age at which a slab experiences construction loads is, of course, lower than the 28-day design strength. Gardner and Poon (1976) had concluded earlier that the tensile and bond strengths of concrete were proportional to the compressive cylinder strength raised to the power 0.8. As shear is governed by tensile strength, it was assumed that shear strength was also related to compressive strength the same way. Data in Table 8.7 were prepared by Gardner (1985) from Klieger's (1958) data, using the 0.8-power criterion to estimate early-age strength as a fraction of the 28-day, 73°F cylinder strength for both Type I normal Portland cement and Type III high-early-strength cement concretes. Gardner (1985) noted that no existing design code specifies a construction load factor. ANSI A10.9-1997 (ANSI, 1997) recommends a load factor of 1.3 for both dead and live construction loads. Kaminetzky and Stivaros (1994) indicated preference for the more conservative load factors required by ACI 318 Appendix C for service conditions—that is, 1.4 and 1.7 for construction dead and live loads, respectively. Gardner used a construction load factor of 1.4 and assumed that the forms have self-weights equal to 10% of the slab self-weight and that the simplified Grundy–Kabaila method is approximately 10% in error. This yielded a factored construction load combination (required strength) of:

TABLE 8.8 Factored Construction Loads on Slabs with Two Shores and Two Reshores

	Age of Slab (Cycles after Casting)							
	1		2		3		4	
Slab	a	b	a	b	a	b	a	b
1	0[a]	0[a]	1.54[a]	1.54[a]	1.54[a]	1.54[a]	1.94	2.37
2	1.54[a]	1.69[a]	2.31[a]	2.31[a]	1.94	2.37	1.94	2.37
3	0.77[a]	0.77[a]	2.37	2.79	1.94	2.37	1.94	2.37
4	1.52	1.94	2.79	3.21	1.94	2.37	1.94	2.37
5	1.10	1.52	2.60	3.01	1.94	2.37	1.94	2.37

[a] Slab supported on grade so construction live load transmission is directly to the ground.
Note: Operation a is removal of lowest level of shores and reshores; operation b is casting of next slab.
Source: Gardner, N.J., *Concrete Int.*, 7(4), 28–34, 1985.

$$U = \left[1.1 \times 1.1 \times 1.4 \times \text{load ratio} + \frac{1}{N}\right] \text{dead load} \tag{8.15}$$
$$\text{(a)}\quad \text{(b)}\quad \text{(c)}\qquad \text{(d)}\qquad \text{(e)}$$

where (a) is error in simplified method, (b) is the weight of the formwork, (c) is the load factor, (d) is the calculated load ratio (Table 8.2), and (e) is an allowance for the construction live load where N is the total number of shore and reshore levels. Using Equation 8.15, the factored construction loads at various stages of construction are shown in Table 8.8 for two levels of shoring and two levels of reshoring. A complete version of Table 8.8 for other combinations of shore and reshore levels is shown in Table 8.9. Gardner (1985) provided the following three examples of safety analysis.

8.4.1.1 Example 8.1

Determine if a flat-slab structure designed for a live-load/dead-load ratio of 1.00 by ACI 318 can be constructed using a two-shore/two-reshore system with a seven-day casting cycle and form stripping one day before casting. Assume an ambient temperature of 73°F and Type I Portland cement concrete:

$$U = D\left[1.4 + 1.7\frac{L}{D}\right] = 3.1D$$

Assuming that the 28-day design strength is equal to the required strength U, the strengths available at various ages of interest are as follows:

Age (days)	Strength Available
6	$0.76 \times 3.1D = 2.36D$
7	$0.79 \times 3.1D = 2.45D$
13	$0.89 \times 3.1D = 2.76D$
14	$0.90 \times 3.1D = 2.79D$
20	$0.96 \times 3.1D = 2.98D$
27	$1.00 \times 3.1D = 3.1D$
28	$1.00 \times 3.1D = 3.1D$

Using the load data from Table 8.8, the adequacy can be checked for every slab at every stage of construction. The results of the check are shown in Table 8.10. It can be seen that the proposed construction scheme overloads slab 4 at ages 13 and 14 days and slab 5 at 14 days. Thus, it cannot be used without modification.

8.4.1.2 Example 8.2

Determine the construction cycle for a slab designed for a live-load/dead-load ratio of 0.5, using one shore plus five reshore levels at a temperature of 55°F. Assume Type I Portland cement concrete and a specified concrete strength of 4000 psi. From Table 8.8, for one level of shores and five levels of reshores, the factored construction loads are 1.86*D* at stripping and 2.15*D* at casting of the next slab. The required strength is:

$$U = D\left[1.4 + 1.7\frac{L}{D}\right] = 2.25D$$

Assuming that the 28-day, 73°F design strength is equal to the required strength *U*, the concrete strength at casting at 55°F needs to be 2.15/2.25 = 96% of the 28-day strength, which occurs at approximately 23 days. The concrete strength at stripping has to be 1.86*D*/2.25*D* = 83%, which occurs at 13 days. In most cases, a 23-day cycle would not be economically acceptable.

8.4.1.3 Example 8.3

Redo the above example to achieve a 7-day placing cycle. The strength of the slab required at casting (7 days) is 0.96 × 4000 psi = 3840 psi; the strength of the slab required at stripping (6 days) is 0.83 × 4000 psi = 3320 psi. To obtain a concrete strength of 3840 psi at 7 days, either the concrete mix must be redesigned or heat must be supplied to accelerate the hydration process. It should be noted that this safety analysis is probably flawed if punching shear governs safety, as it usually does for slab systems without column-line beams. This is for two important reasons. First, as mentioned earlier, simplified Grundy–Kabaila-type analysis cannot lead to accurate estimates of punching shear forces at slab–column joints. Second, the assumption that punching shear strength varies with the 28-day compressive cylinder strength of concrete raised to the power 0.8 was not verified in later tests by Gardner (1960), who found punching shear strength to vary with the cube root of the 28-day compressive cylinder strength.

8.4.2 Refined Safety Analysis

A more refined safety analysis was carried out by Kaminetzky and Stivaros (1994) on a test multistory flat-plate office building (Figure 8.39), assumed to have been designed according to ACI 318 with a 50-psf (2.4 kPa) live load and an additional superimposed partition load of 30 psf (1.5 kPa). This example assumed one level of shores and three levels of reshores with a construction rate of two floors per week. It is also assumed that the shores and reshores were removed and relocated a day before casting the top slab. A 50-psf (2.4 kPa) construction live load was assumed to be present only during the placement of concrete in the top slabs. The *in situ* concrete strength can be estimated by testing field-cured cylinders in combination with other available nondestructive methods. Figure 8.40 shows the assumed compressive strength–time relationship for two different construction temperatures: 55 and 73°F.

Stivaros' computer program (Stivaros and Halvorsen, 1990), based on the equivalent frame method of analysis, was employed to evaluate the construction load distribution between the shoring system and the concrete frame. The program, as mentioned earlier, builds the structure from the first floor to the roof and evaluates the loads on each floor slab and the support system for every construction stage. The punching shear stresses due to applied loads are also computed at each column location for every construction step. The program provides the available load-carrying capacities of the slabs and the available punching shear strengths of slab–column connections at the time of application of the construction loads; thus, a safety comparison can be made. The load-carrying capacities are based on flexural considerations, accounting for partially developed concrete compressive strength. A key assumption is that the load factors and strength-reduction factors used for the design of the slabs for service conditions are the same for the construction stage as well. The available punching shear strength is evaluated according to ACI 318 (ACI Committee 318, 2005) and is equal to $\sqrt{F_{ct}}$, where $\phi = 0.85$, and F_{ct} is the available concrete strength at the time the load is applied. The results of the construction load analysis are shown in Figure 8.41 and Figure 8.42. The figures show the maximum factored slab loads (normalized

TABLE 8.9 Factored Construction Loads with Cycles of Construction

		Construction Cycle													
		1		2		3		4		5		6		7	
	Slab	a	b	a	b	a	b	a	b	a	b	a	b	a	b
1 Form, 0 reshore	1	1.54	3.94												
	2	1.54	3.94												
	3	1.54	3.94												
1 Form, 1 reshore	1	1.54	1.54	2.19	3.04										
	2	2.19	3.04	2.19	3.04										
	3	2.19	3.04	2.19	3.04										
1 Form, 2 reshores	1	1.54	1.54	1.54	1.54	2.02	2.60								
	2	1.54	1.54	2.02	2.60	2.02	2.60								
	3	2.02	2.60	2.02	2.60	2.02	2.60								
1 Form, 3 reshores	1	1.54	1.54	1.54	1.54	1.54	1.54	1.94	2.37						
	2	1.54	1.54	1.54	1.54	1.94	2.37	1.94	2.37						
	3	1.54	1.54	1.94	2.37	1.94	2.37	1.94	2.37						
	4	1.94	2.37	1.94	2.37	1.94	2.37	1.94	2.37						
1 Form, 4 reshores	1	1.54	1.54	1.54	1.54	1.54	1.54	1.54	1.54	1.89	2.23				
	2	1.54	1.54	1.54	1.54	1.54	1.54	1.89	2.23	1.89	2.23				
	3	1.54	1.54	1.54	1.54	1.89	2.23	1.89	2.23	1.89	2.23				
	4	1.54	1.54	1.89	2.23	1.89	2.23	1.89	2.23	1.89	2.23				
	5	1.89	2.23	1.89	2.23	1.89	2.23	1.89	2.23	1.89	2.23				
1 Form, 5 reshores	1	1.54	1.54	1.54	1.54	1.54	1.54	1.54	1.54	1.54	1.54	1.86	2.15		
	2	1.54	1.54	1.54	1.54	1.54	1.54	1.54	1.54	1.86	2.15	1.86	2.15		
	3	1.54	1.54	1.54	1.54	1.54	1.54	1.86	2.15	1.86	2.15	1.86	2.15		
	4	1.54	1.54	1.54	1.54	1.86	2.15	1.86	2.15	1.86	2.15	1.86	2.15		
	5	1.54	1.54	1.86	2.15	1.86	2.15	1.86	2.15	1.86	2.15	1.86	2.15		
	6	1.86	2.15	1.86	2.15	1.86	2.15	1.86	2.15	1.86	2.15	1.86	2.15		
2 Forms, 0 reshore	1	0	0	2.19	3.04										
	2	2.19	3.04	3.46	4.31										
	3	0.92	1.77	2.84	3.68										
	4	1.55	2.40	3.14	3.99										
	5	1.25	2.09												
	—[a]	1.35	2.19	3.04	3.89										

2 Forms, 1 reshore	1	0	0	1.54	1.54	2.03	2.60								
	2	1.54	1.54	2.87	3.43	2.03	2.60								
	3	1.18	1.74	2.74	3.30	2.03	2.60								
	4	1.32	1.87	2.81	3.37	2.03	2.60								
	5	1.25	1.81	2.77	3.33	2.03	2.60								
	6	1.28	1.84	2.79	3.35	2.02	2.60								
	—[a]	1.27	1.82	2.81	3.37	2.03	2.60								
2 Forms, 2 reshores	1	0	0	1.54	1.54	1.54	1.54	1.94	2.37						
	2	1.54	1.69	2.31	2.31	1.94	2.37	1.94	2.37						
	3	0.77	0.77	2.37	2.79	1.94	2.37	1.94	2.37						
	4	1.52	1.94	2.79	3.21	1.94	2.37	1.94	2.37						
	5	1.10	1.52	2.59	3.01	1.94	2.37	1.94	2.37						
	6	1.30	1.72	2.69	3.11	1.94	2.37	1.94	2.37						
	7	1.20	1.62	2.64	3.06	1.94	2.37	1.94	2.37						
	—[a]	1.23	1.66	2.66	3.08	1.94	2.37	1.94	2.37						
2 Forms, 3 reshores	1	0	0	1.54	1.54	1.54	1.54	1.54	1.54	1.89	2.23				
	2	1.54	1.54	2.31	2.31	1.54	1.54	1.89	2.23	1.89	2.23				
	3	0.77	0.77	1.93	1.93	1.89	2.23	1.89	2.23	1.89	2.23				
	4	1.16	1.16	2.54	2.88	1.89	2.23	1.89	2.23	1.89	2.23				
	5	1.25	1.59	2.59	2.93	1.89	2.23	1.89	2.23	1.89	2.23				
	6	1.20	1.54	2.57	2.91	1.89	2.23	1.89	2.23	1.89	2.23				
	7	1.22	1.55	2.57	2.91	1.89	2.23	1.89	2.23	1.89	2.23				
	—[a]	1.22	1.55	2.57	2.90	1.89	2.23	1.89	2.23	1.89	2.23				
2 Forms, 4 reshores	1	0	0	1.54	1.54	1.54	1.54	1.54	1.54	1.54	1.54	1.86	2.14		
	2	1.54	1.54	1.54	1.54	1.54	1.54	1.54	1.86	2.14	2.14	1.86	2.14		
	3	0.77	0.77	1.93	1.93	1.54	1.54	1.86	2.14	1.86	2.14	1.86	2.14		
	4	1.16	1.16	2.13	2.13	1.86	2.14	1.86	2.14	1.86	2.14	1.86	2.14		
	5	0.95	0.95	2.39	2.66	1.86	2.14	1.86	2.14	1.86	2.14	1.86	2.14		
	6	1.34	1.61	2.59	2.86	1.86	2.14	1.86	2.14	1.86	2.14	1.86	2.14		
	7	1.13	1.40	2.49	2.76	1.86	2.14	1.86	2.14	1.86	2.14	1.86	2.14		
	—[a]	1.20	1.47	2.52	2.79	1.86	2.14	1.86	2.14	1.86	2.14	1.86	2.14		
2 Forms, 5 reshores	1	0	0	1.54	1.54	1.54	1.54	1.54	1.54	1.54	1.54	1.54	1.54	1.84	2.07
	2	1.54	1.54	1.54	1.54	1.54	1.54	1.54	1.54	1.54	1.54	1.84	2.07	1.84	2.07
	3	0.77	0.77	1.93	1.93	1.54	1.54	1.54	1.54	1.84	2.07	1.84	2.07	1.84	2.07
	4	1.16	1.16	2.13	2.13	1.54	1.54	1.84	2.07	1.84	2.07	1.84	2.07	1.84	2.07
	5	0.95	0.95	2.02	2.02	1.84	2.07	1.84	2.07	1.84	2.07	1.84	2.07	1.84	2.07
	6	1.06	1.06	2.43	2.67	1.84	2.07	1.84	2.07	1.84	2.07	1.84	2.07	1.84	2.07
	7	1.24	1.48	2.51	2.75	1.84	2.07	1.84	2.07	1.84	2.07	1.84	2.07	1.84	2.07
	—[a]	1.19	1.43	2.48	2.72	1.84	2.07	1.84	2.07	1.84	2.07	1.84	2.07	1.84	2.07

[a] Converged.

Source: Gardner, N.J., *Concrete Int.*, 7(4), 28–34, 1985.

to the self-weight of the slab) and punching shear stresses that occurred on the floor slabs during construction. Also shown in the figures are the load-carrying capacities (allowable loads) and allowable punching shear stresses of the concrete slabs at two temperature conditions: 55 and 73°F. Figure 8.41 shows that the maximum applied factored load, which occurred on 4-day-old slabs, exceeded the allowable loads

TABLE 8.10 Comparison of Strength and Factored Load for Worked Example

Age After Casting	Strength Available	Load Applied				
		Slab 1	Slab 2	Slab 3	Slab 4	Slab 5
6	2.36	0	1.54	0.77	1.52	1.10
7	2.45	0	1.69	0.77	1.94	1.52
13	2.76	1.54	2.31	2.37	2.79	2.60
14	2.79	1.54	2.31	2.79	3.21	3.01
20	2.98	1.54	1.94	1.94	1.94	1.94
21	2.98	1.54	2.37	2.37	2.37	2.37
27	3.10	1.94	1.94	1.94	1.94	1.94
28	3.10	2.37	2.37	2.37	2.37	2.37

Source: Gardner, N.J., *Concrete Int.*, 7(4), 28–34, 1985.

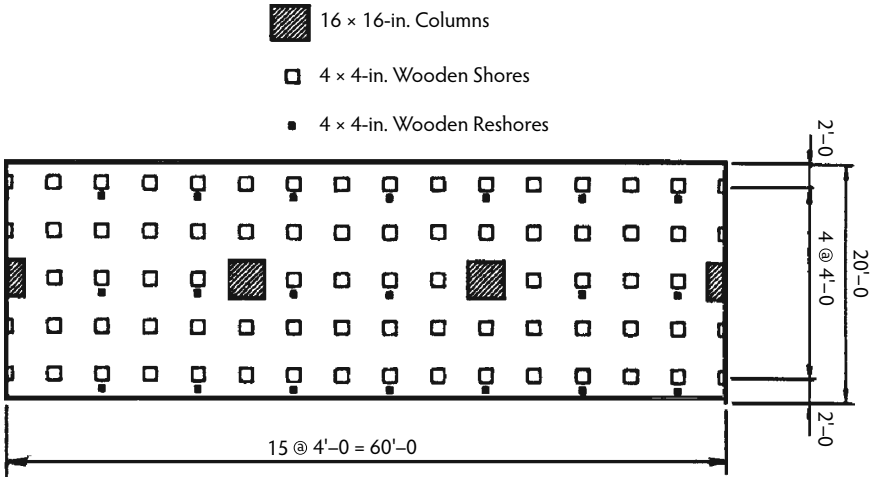

FIGURE 8.39 Typical floor plan of construction example studied by Kaminetzky (1994).

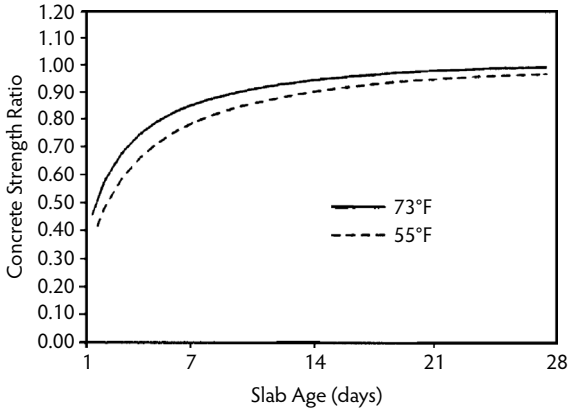

FIGURE 8.40 Compressive strength development vs. time assumed by Kaminetzky (1994).

for both temperature conditions. This means that the proposed construction scheme cannot be safely executed. Similar unsafe construction conditions are shown in Figure 8.42, where the punching shear stresses due to the applied loads exceeded the allowable stresses. For this particular example, the available strengths in both flexure and shear have been exceeded; however, because of the possibility of inelastic redistribution of bending moments and because of the improbabilities of any redistribution of punching shear stresses, a sudden shear failure is likely to occur prior to flexural failure. Kaminetzky and Stivaros (1994) pointed out that had some floors of the above building been designed for an additional live load of 20 psf (1.0 kPa), the slabs would have been flexurally adequate to carry the construction loads for the 73°F temperature condition at a rate of two floors per week (Figure 8.43). Also, a construction rate of one floor per week would have been safe even for the 55°F temperature condition; however, the construction operation still could not proceed safely because of the punching shear deficiency of the slabs.

8.5 Serviceability Consequences of Construction Loads

Floors in residential as well as office buildings are often made of thin, solid concrete slabs with two-way reinforcement. The trend in recent years has been toward a progressive decrease in the ratio of the thickness of slab to length of span. This obviously causes a corresponding reduction in the flexural rigidity

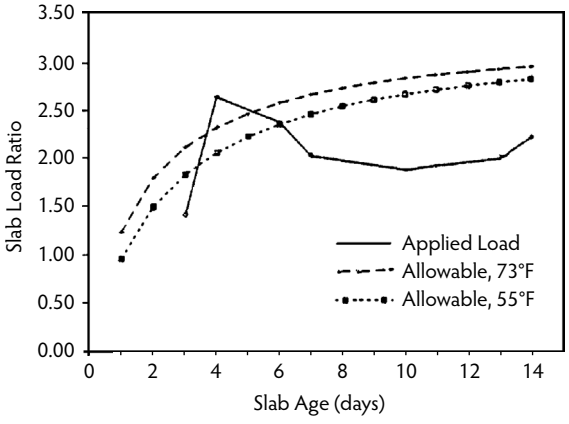

FIGURE 8.41 Allowable and applied slab loads from Kaminetzky's (1994) analysis (live load = 50 psf).

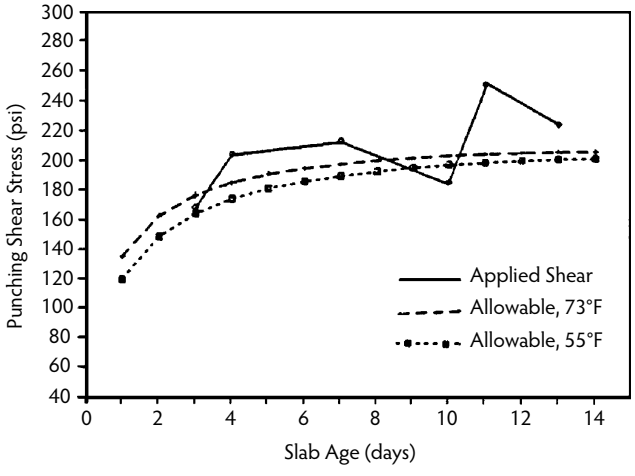

FIGURE 8.42 Allowable and applied punching shear stress from Kaminetzky's (1994) analysis.

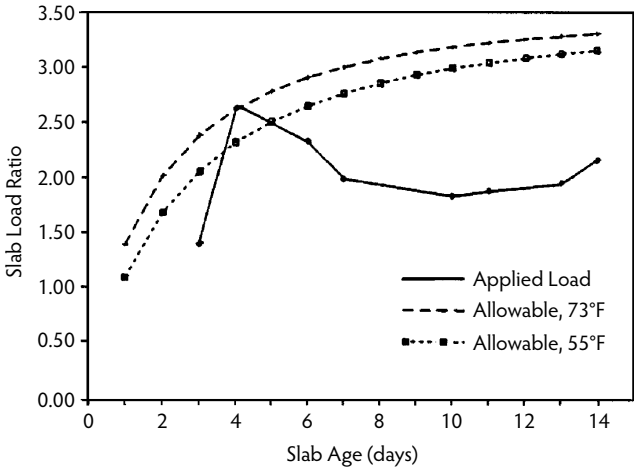

FIGURE 8.43 Allowable and applied slab loads from Kaminetzky's (1994) analysis (live load = 70 psf).

of slabs. The consequent deformations have not always received as much attention as preventing collapse. Large permanent deformations of floor slabs have sometimes resulted. Whereas such deformations are often aesthetically unacceptable, their effects may also be seriously disturbing from a practical point of view. Cracking of brick partitions, jamming of doors, and cracking of windows have not been uncommon. At least in one reported case, long-term deflection of an interior span of a floor caused an adjacent balcony to slope inward. Rain falling on the balcony ran inward under the doorway and formed a pool in the middle of the floor, damaging carpets. Excessive long-term deflections of slabs are clearly to be avoided.

8.5.1 Causes of Excessive Deflections

Excessive deflections can sometimes be attributed to a single cause. More commonly, however, the problem may be traced to a combination of several contributing factors. Potential problem areas include design, construction, materials, environmental conditions, and change in occupancy (Scanlon, 1987).

8.5.1.1 Design

The single most common cause of large deflections associated with design is the selection of a slab thickness that is too small for the spans used. Another common problem is inadequate flexural reinforcement; as a result, premature yielding may occur, causing a substantial loss of flexural stiffness and leading to excessive deflection.

8.5.1.2 Materials

Higher than normal creep and shrinkage characteristics have been identified as contributing factors in cases of large deflections reported in Australia. While achieving high concrete strengths, high-shrinkage characteristics have sometimes been produced; the increase in slab warping has more than offset the benefits obtained from the increase in the modulus of elasticity of the concrete. In post-tensioned slabs, higher than normal prestress losses may lead to unanticipated deflections. Alkali–aggregate reactions produced by certain types of aggregate and cement may cause cracking that can adversely affect flexural stiffness.

8.5.1.3 Environmental Conditions

For slab surfaces exposed to daily or seasonal temperature fluctuations, temperature gradients set up through the member thickness may lead to unanticipated deflections.

8.5.1.4 Change in Occupancy

Slabs adequately designed and constructed for the original design loading may suffer deflection problems if the occupancy changes and if the change involves an increase in the sustained load applied to the slab.

8.5.1.5 Construction

The following is a list of factors, as compiled by Taylor and Heiman (1977), that contribute to excessive long-term slab deflections:

1. Formwork has not been cambered in cantilevers and large interior panels, so even early deflections are obvious.
2. Slabs have been supported by props bearing on sole plates that were of inadequate size to prevent appreciable settlement into the ground surface and hence induced slab deformation before stripping.
3. Construction loading from propping or the storage of materials during the early life of the slabs has been severe enough to cause extensive slab cracking and hence loss of stiffness.
4. Top reinforcement at supporting elements has been pushed down during slab construction, substantially reducing its effective depth and hence reducing the contribution made to slab stiffness by continuity at supports.
5. Curing has in many instances been inadequate and has sometimes led to insufficient strength development and excessive shrinkage cracking.

Item 4 above is a surprisingly common occurrence. Quite often, the top steel over supports is not securely held in place and is displaced toward the neutral axis, greatly reducing the stiffness over the support. If the effective depth is 7 in. instead of 8 in., as has been observed, the stiffness is reduced by 23%, and the member tends to behave as if it were simply reinforced.

Discussion here obviously needs to focus on the very important item 3 above. As noted earlier, when the shore/reshore method of multistory building construction is used, high-early-age, short-duration loads are imposed on the floor slabs. These loads can be comparable in magnitude to, or even exceed, the design service loads and are applied to concrete slabs that have not achieved their specified concrete strength. Because the slab concrete is immature with a reduced modulus of elasticity (see preceding section), the immediate deflections due to the construction loads are relatively large. Creep effects may be looked upon as being dependent upon the magnitude of the applied stress relative to the developed concrete strength; hence, creep deflections due to construction loads are also large. Deflection due to concrete shrinkage must also be considered.

8.5.2 Components of Long-Term Deflection

Shrinkage and creep are the two primary contributors to long-term deflections of reinforced concrete members. Shrinkage produces a shortening of the concrete in a member that is resisted by the reinforcing steel. The magnitude of shrinkage curvature (Figure 8.44b) depends on the amount of nonsymmetry of reinforcement and on the relative areas of concrete and steel in a reinforced concrete member. These shrinkage curvatures, which are the greatest for beams with tension reinforcement only, generally have the same sign as those due to moments produced by transverse loads, and thus they magnify the deflection due to load.

Considering creep alone, the increase in strain with time will be as shown by line B in Figure 8.45b, while line A indicates the strain distribution immediately on application of the load. Strain at the extreme fiber in compression increases considerably, while the strain at the level of the steel changes very little. As this occurs, the compressive stresses in the concrete are reduced (Figure 8.45c) because the neutral axis moves toward the reinforcement, and the steel stresses increase because the internal lever arm shortens. It can be seen from Figure 8.45b that the relative increase in curvature caused by creep is less than the relative increase in strain due to creep. Thus, the relative increase in deflection is also less than the increase in strain due to creep.

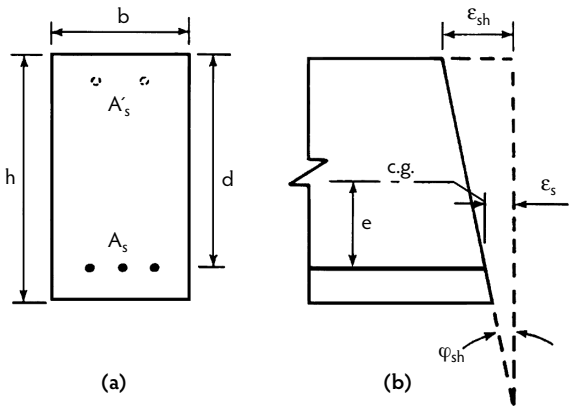

FIGURE 8.44 Shrinkage curvature of a section of a reinforced concrete flexural member.

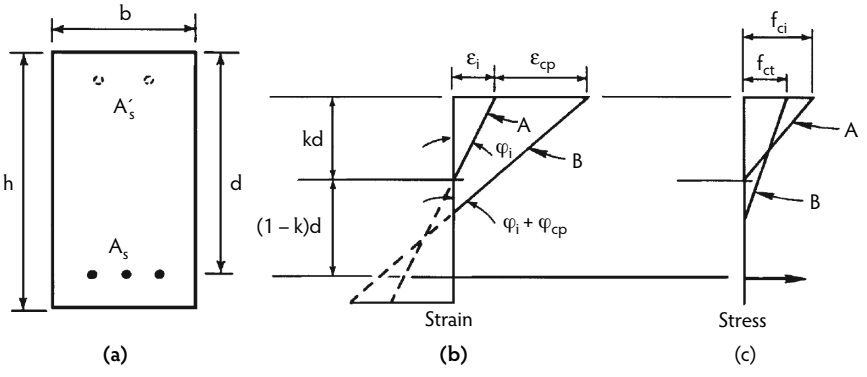

FIGURE 8.45 Strain and stress distribution and curvature due to initial and creep deformation in a section of a reinforced concrete flexural member.

In addition to the difficulty of determining the creep-time history of a particular concrete under constant, uniformly distributed sustained stress, a reinforced concrete flexural member is subjected to a nonuniform stress distribution and often a variable load history. A detailed analysis of the effects of a variable stress history, even for uniformly loaded members, is usually not feasible, and shorter, more appropriate methods are used. One such method uses a reduced or effective modulus called the *sustained modulus of elasticity*, which refers to concrete under a constant sustained stress:

$$E_{ct} = \frac{\sigma_{\text{constant}}}{\epsilon_{\text{initial}} + \epsilon_{\text{creep},t}} = \frac{\sigma_{\text{constant}}}{(1+C_t)\,\epsilon_{\text{initial}}} = \frac{E}{1+C_t} \tag{8.16}$$

where $C_t = \epsilon_{\text{creep}}/\epsilon_{\text{initial}}$ is the creep coefficient at time t, the ultimate value of which may be denoted by C_u. It may be parenthetically noted that in considering creep deformations, use of the specific creep strain δ_t (creep per unit stress) or creep coefficient C_t (ratio of creep strain to initial strain) yields the same results (ACI Committee 209, 1971), as:

$$C_t = \delta_t E_{ci} \tag{8.17}$$

This can be seen from the following relations: creep strain at time $t = (\sigma_{\text{constant}})\delta_t = (\epsilon_{\text{initial}})C_t$, and $E_{ci} = \sigma_{\text{constant}}/\epsilon_{\text{initial}}$. The choice of δ_t or C_t is a matter of convenience, depending on whether applying the creep factor to stress or strain is desired.

With reference to Figure 8.45 and the earlier discussion on that figure,

$$\frac{\Delta_{\text{creep},t}}{\Delta_{\text{initial}}} = \frac{\phi_{\text{creep},t}}{\phi_{\text{initial}}} = k_{rc}\frac{\epsilon_{\text{creep},t}}{\epsilon_{\text{initial}}} = k_{rc}C_t \tag{8.18}$$

provided that the same moment of inertia is used in the computation of short- and long-term deflections. The factor k_{rc} accounts for the effect of compression steel and the offsetting effects of a downward movement of the neutral axis due to creep strain distribution and upward movement of the neutral axis due to progressive cracking under creep loading (plus the small effect, if any, of repeated live-load cycles). These offsetting effects normally appear to result in a downward movement of the neutral axis, such that k_{rc} is less than unity.

Because shrinkage and creep deflections are additive, their combined value is often estimated in approximate calculations with a single time-dependent factor applied to the initial deflection:

$$\Delta_t = k_r T_t \Delta_{\text{initial}} \tag{8.19}$$

where T_t is a multiplier for additional long-term deflections due to creep and shrinkage, the ultimate value of which may be denoted by T_u. The factor k_r in Equation 8.19 and the factor k_{rc} in Equation 8.18 serve largely the same purpose. The following values have been suggested for the two factors (ACI Committee 209, 1971):

$$k_{rc} = 0.85 - 0.45(A_s'/A_s) \geq 0.40 \tag{8.20}$$

$$k_{rc} = 1.00 - 0.60(A_s'/A_s) \geq 0.40 \tag{8.21}$$

ACI 318 (ACI Committee 318, 2005) basically takes the Equation 8.19 approach to estimating long-term deflections.

The opportunity usually does not arise for temperature to influence deflections of floor systems, as these are usually protected from large temperature changes soon after casting. In slabs that are not so protected, temperature changes can be important. Because the thermal coefficients of steel and concrete are roughly the same, little if any curvature results from temperature changes that are uniform across a section of a member. With regard to differential temperatures (such as inside vs. outside temperatures of heated or cooled buildings), the deformation of reinforced concrete members is similar to or opposite that due to shrinkage; for example, the deflection would be downward in the case of roofs of heated buildings and upward in the case of roofs of air-conditioned buildings (Branson, 1977).

Because shrinkage is independent of load, it appears illogical for deflection directly caused by shrinkage to be related to load via the initial deflection; there is, however, an indirect way in which shrinkage can influence deflection. The stiffness of a cracked reinforced concrete section is usually less—sometimes much less—than the stiffness of the surrounding gross concrete section. It would appear that this change from an uncracked to a cracked section, which may be brought about and extended over a considerable period by shrinkage (plus creep and thermal) effects, offers the potential for a corresponding continuing increase in deflection. Branson (1987) cited laboratory tests by others to indicate that the formation of new cracks during sustained loading depends on the development of earlier cracks during the initial loading stage. For example, in beams with a low 0.60% steel and a steel stress $f_s = 20$ ksi at initial loading, about half the cracks occurred upon initial loading and the remainder during the sustained loading. In beams with the same low steel percentage but $f_s = 30$ ksi, almost all cracks occurred upon initial loading. In beams with a higher 2.0% steel, cracks appeared rather early, with little additional cracking occurring during the sustained loading. According to Branson, this effect, which would seem to require the use of a $k_r > 1$ in Equation 8.19, is for most practical purposes taken into account through the use of a suitable effective moment of inertia in initial deflection calculations and through the use of the k_r factor as given by Equation 8.21.

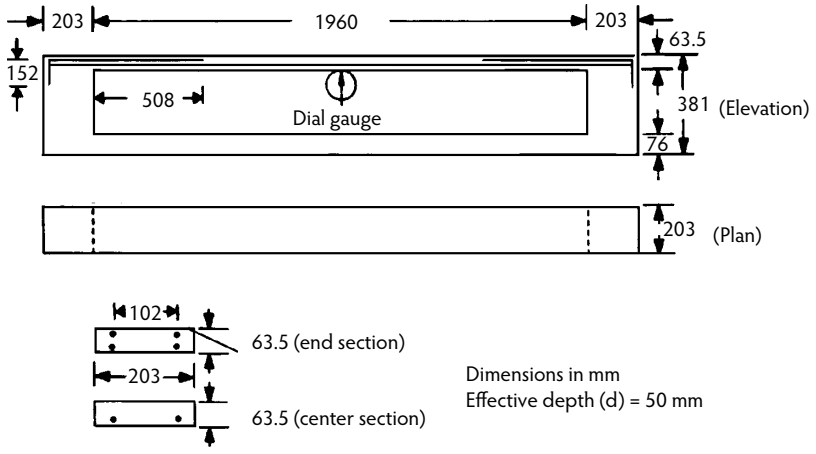

FIGURE 8.46 Details of one-way slab models tested by Fu and Gardner. (From Fu, H.C. and Gardner, N.J., in *Properties of Concrete at Early Ages*, SP-95, American Concrete Institute, Farmington Hills, MI, 1986, pp. 173–200.)

8.5.3 Experimental Investigation

Fu and Gardner (1986) fabricated five nominally identical single-span one-way slabs. All of the slabs (Figure 8.46) were 8 in. (203 mm) wide and 2.5 in. (64 mm) deep, spanned 77 in. (1960 mm), were reinforced with 5-mm diameter wires in one direction, and were cast from the same mix. Ready-mixed concrete with a target 28-day strength of 4000 psi (28 MPa) was used. Only the midspan deflections of the five one-way slabs were measured under load. After the formwork was stripped, measurements were made every day for the first month and then weekly afterward. In addition, shrinkage of four concrete prisms, compressive strength, and modulus of elasticity of the concrete were also measured. The five slabs were subjected to different load histories during the first 28 days after casting. Slabs 1 and 2 were subjected to simplified load histories, while slabs 3, 4, and 5 were subjected to load histories typical of one shore plus two reshores, one shore plus two levels of preshores (this term is discussed later), and three levels of shores. The load histories are given in Figure 8.47. The measured deflections are given in Figure 8.48a for the first 28 days and Figure 8.48b for the first 489 days. An examination of the deflection curves in Figure 8.48a reveals that the slopes of all these curves were virtually the same after day 28; subsequent deflections after removal of the construction loads seemed to be independent of prior loading. In other words, the additional deflections due to creep and shrinkage of concrete during the first 28 days of loading could not be recovered despite removal of the construction loads and even though identical loads were sustained on the slabs afterward. The net deflections after 28 days, taken as the sum of deflections due to loading (plus) and unloading (minus) alone and excluding deflections due to creep and shrinkage, were measured to be 0.60, 0.63, 0.62, 0.60, and 0.58 mm for slabs 1 to 5, respectively. It is equally interesting to note that the increases in deflections from day 28 to the end of the observation period (say, 489 days) for all five slabs were very close indeed: 1.60, 1.41, 1.49, 1.50, and 1.57 mm for slabs 1 to 5, respectively. However, due to the distinct loading histories in the initial stages, the corresponding final deflections after 489 days were 3.26, 4.13, 3.32, 3.51, and 4.31 mm, giving ratios of final deflection to net deflection at 28 days of 5.43, 6.56, 5.35, 5.85, and 7.43.

8.5.4 Control of Slab Deflections

The state of the art for control of two-way slab deflections was reviewed in ACI Committee 435 (1995). The methods of calculating slab deflections were presented, and the effects of two-way action, cracking, creep, shrinkage, and construction loads were considered. Probably the surest way to control deflections is to carefully sequence the operations of shore removal and reshoring. With a column layout like the one shown in Figure 8.49, stringers would normally be run in the short direction at about 4 ft on-center,

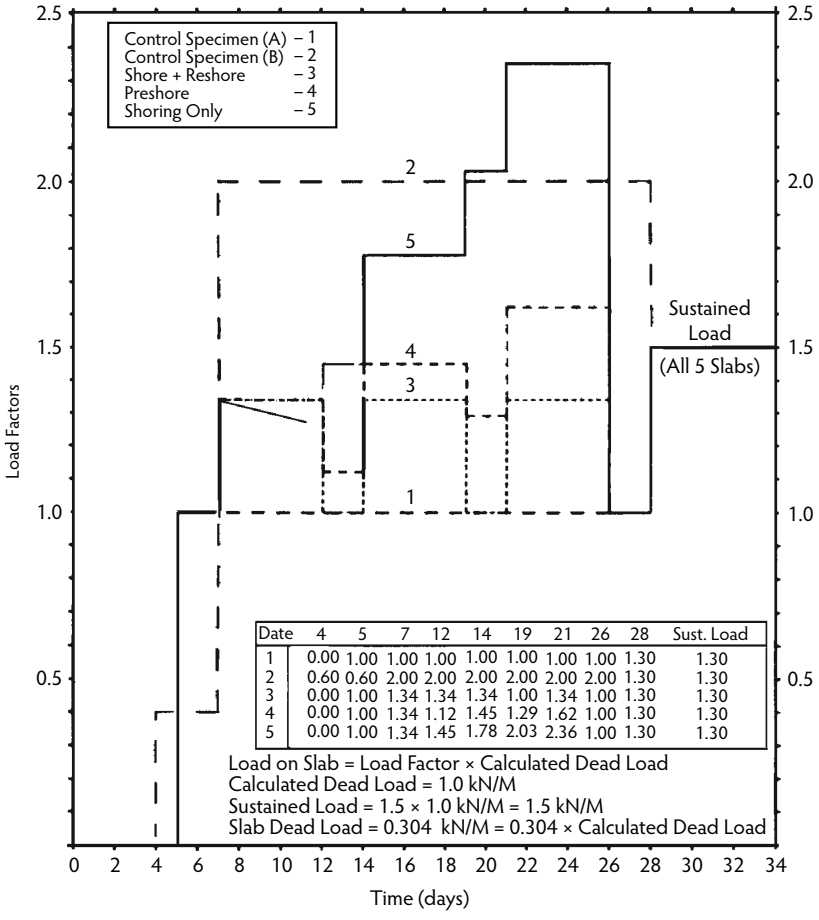

Date	4	5	7	12	14	19	21	26	28	Sust. Load
1	0.00	1.00	1.00	1.00	1.00	1.00	1.00	1.00	1.30	1.30
2	0.60	0.60	2.00	2.00	2.00	2.00	2.00	2.00	1.30	1.30
3	0.00	1.00	1.34	1.34	1.34	1.00	1.34	1.00	1.30	1.30
4	0.00	1.00	1.34	1.12	1.45	1.29	1.62	1.00	1.30	1.30
5	0.00	1.00	1.34	1.45	1.78	2.03	2.36	1.00	1.30	1.30

FIGURE 8.47 Loading histories on slab models tested by Fu and Gardner. (From Fu, H.C. and Gardner, N.J., in *Properties of Concrete at Early Ages*, SP-95, American Concrete Institute, Farmington Hills, MI, 1986, pp. 173–200.)

supported on shores. Ribs or purlins would then be run in the orthogonal direction, also at about 4 ft on-center, supported on the stringers. Finally, the 4 ft × 8-ft plywood sheets would be supported on the ribs. It has been suggested (Cantor and Rizzi, 1982), on the basis of successful experience with flat-plate buildings in the New York area, that alternate plywood sheets in both the long and the short direction (shown shaded in Figure 8.49) should be supported directly by extra shores (indicated by x in Figure 8.49). These latter shores (attached to the plywood rather than to the stringers as the other shores are), also called *preshores* or permanent shores, may be installed at the time the other shores are installed or just before shore removal. When the time comes for removal of formwork, a day or two after casting or when concrete strength reaches a certain minimum value, the regular shores, the stringers, the purlins, and the plywood sheets that are not directly held by the extra shores can all be removed. Before the extra shores and the plywood sheets held by them are removed, however, reshores should be installed at about 8 ft on-center directly to the concrete slab. The extra shores or preshores should be removed only after the reshores have been installed.

The above scheme of removing the shores and installing the reshores does not permit more than 8 ft of slab span to be left unsupported at any time until the slab is sufficiently mature. With such short unsupported slab spans, slab deflections under usual circumstances cannot assume disturbing proportions, however high the loading may be during construction and however immature the slab may be when it is called upon to support those loads.

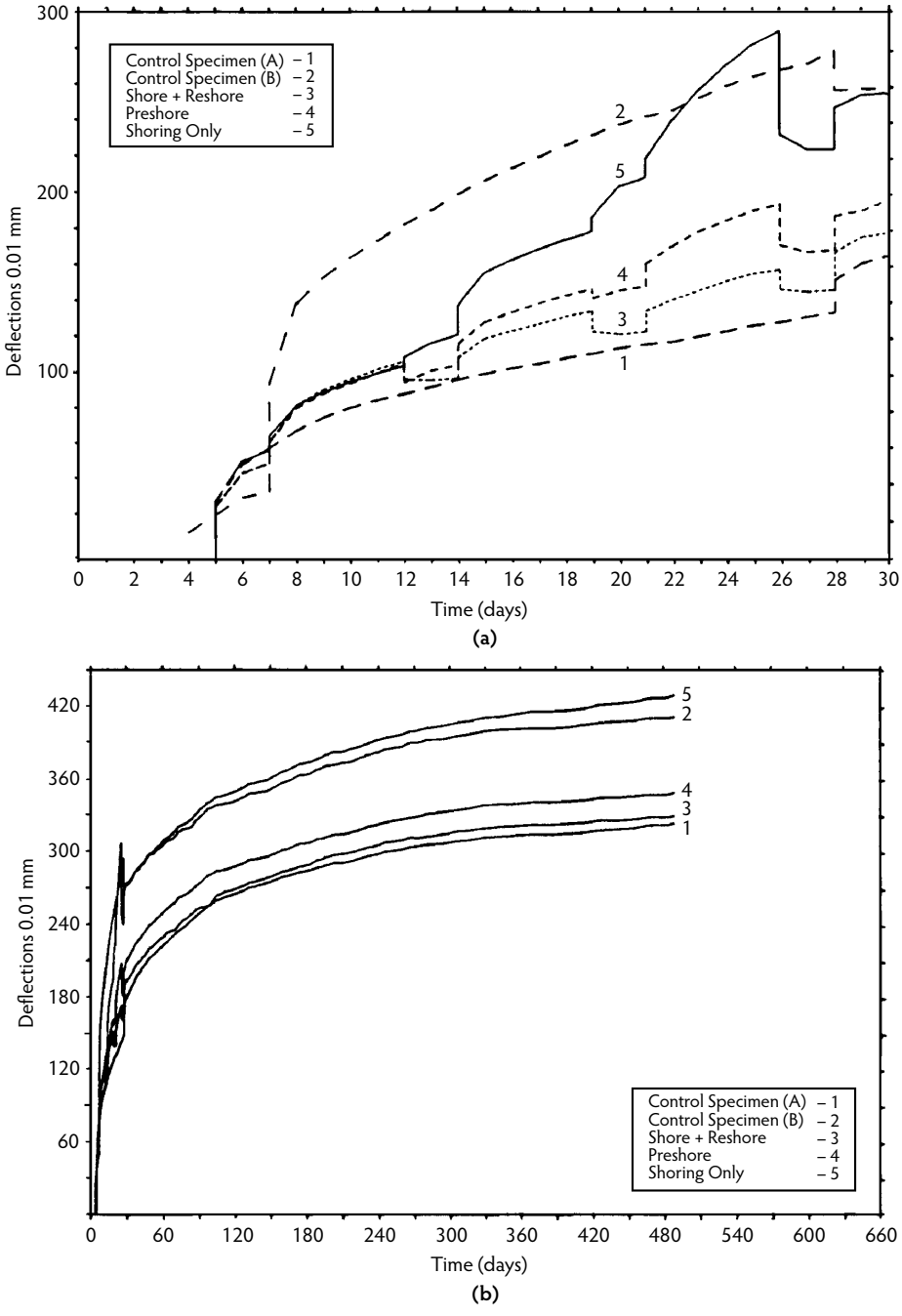

FIGURE 8.48 Deflections due to construction loads measured in slab models tested by Fu and Gardner. (From Fu, H.C. and Gardner, N.J., in *Properties of Concrete at Early Ages*, SP-95, American Concrete Institute, Farmington Hills, MI, 1986, pp. 173–200.)

The above consideration applies for the use of flying forms also. Figure 8.50 shows a reinforced concrete slab supported on reinforced concrete columns spaced at 20 ft on-center in both directions. With such a column layout, an 18-ft-wide form table would normally be used; however, in that case, as soon as the

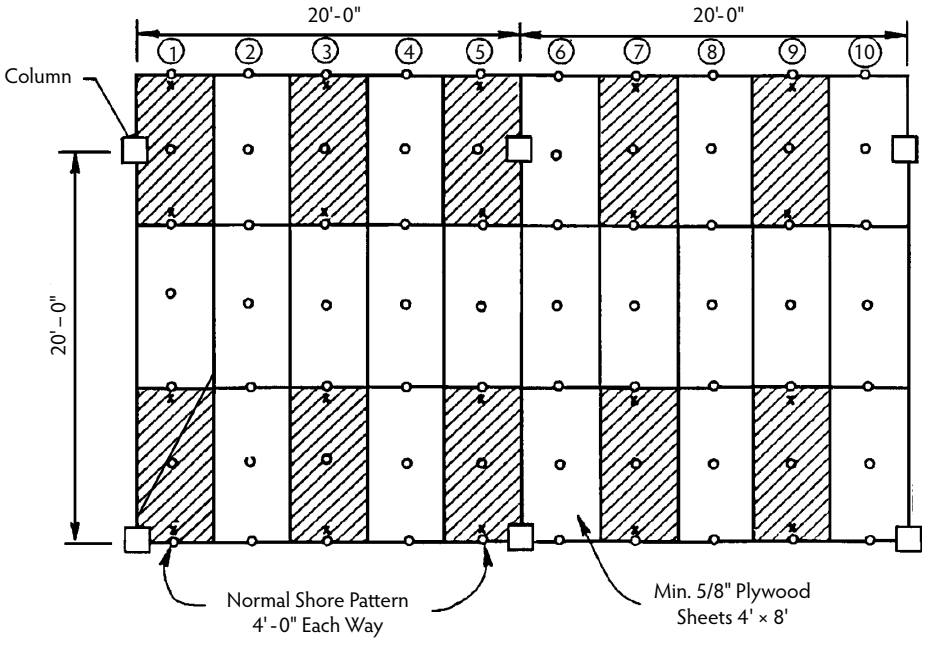

FIGURE 8.49 Sequence of shore removal and reshoring that restricts the slab span left unsupported at an early age. (From Cantor, I.G. and Rizzi, A.V., in *Proceedings of the First International Conference on Forming Economical Concrete Buildings*, Lincolnshire, IL, November 8–10, Portland Cement Association, Skokie, IL, 1982, pp. 18.1–18.12.)

flying form is removed 18 ft of slab span would be left unsupported. If deflections are of concern, two 8-ft-wide form tables, with a filler strip of formwork in between, may be used instead. With the narrower form tables, even when they are removed no more than 8 ft of slab span would be left unsupported. Admittedly, two 8-ft-wide form tables with a filler strip of formwork are significantly more expensive than a single 18-ft-wide form table. The added expense has to be weighed carefully against any advantage that is to be gained in terms of reduced deflections.

8.6 Codes and Standards

The following documents have been mentioned in this chapter:

1. *Guide to Formwork for Concrete*, ACI 347-04 (American Concrete Institute, Farmington Hills, MI)
2. *American National Standard for Construction and Demolition Operation–Concrete and Masonry Work–Safety Requirements*, ANSI A10.9-1997 (American National Standards Institute, New York)

The first of the items is an ACI committee report, and the second is an ANSI standard. Neither of the two is adopted into the International Building Code (IBC), the model code that increasingly forms the basis of the legal codes of various local jurisdictions (cities, counties, and states) within the United States. The latest edition of the IBC, dated 2006, adopts the 2005 edition of ACI Committee 318 *Building Code Requirements for Structural Concrete* for regulations concerning concrete design and construction. This edition of the standard contains interesting and important provisions related to the loading imposed on a concrete structure during construction. These provisions are discussed below. It should also be mentioned that the ASCE Standards Committee on Design Loads during Construction has issued a relatively new standard, ASCE/SEI 37-02 (*Design Loads on Structures during Construction*).

For the first time, the 1995 edition of the ACI 318 standard contained the following requirements, which have remained unchanged through the 2005 edition and are directly quoted from the standard:

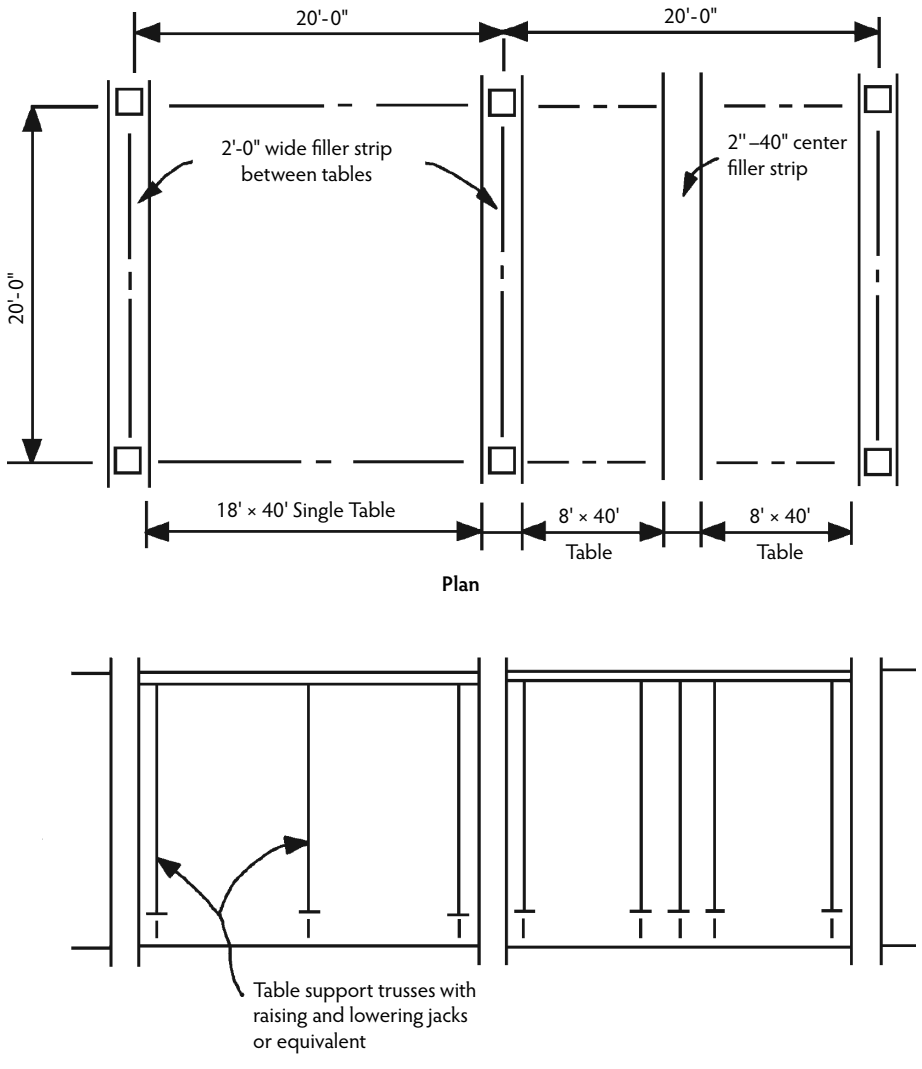

FIGURE 8.50 Restriction on slab span left unsupported at an early age with the use of flying forms. (From Cantor, I.G. and Rizzi, A.V., in *Proceedings of the First International Conference on Forming Economical Concrete Buildings*, Lincolnshire, IL, November 8–10, Portland Cement Association, Skokie, IL, 1982, pp. 18.1–18.12.)

ACI 318 §6.2. Removal of forms, shores, and reshoring

ACI 318 §6.2.1. Removal of forms

Forms shall be removed in such a manner as not to impair safety and serviceability of the structure. Concrete to be exposed by form removal shall have sufficient strength not to be damaged by removal operation.

ACI 318 §6.2.2. Removal of shores and reshoring

The provisions of ACI 6.2.2.1 through ACI 6.2.2.3 shall apply to slabs and beams except where cast on the ground.

ACI 318 §6.2.2.1. Before starting construction, the contractor shall develop a procedure and schedule for removal of shores and installation of reshores and for calculating the loads transferred to the structure during the process.

(a) The structural analysis and concrete strength data used in planning and implementing form removal and shoring shall be furnished by the contractor to the building official when so requested;

(b) No construction loads shall be supported on, nor any shoring removed from, any part of the structure under construction except when that portion of the structure in combination with remaining forming and shoring system has sufficient strength to support safely its weight and loads placed thereupon;

(c) Sufficient strength shall be demonstrated by structural analysis considering proposed loads, strength of forming and shoring system, and concrete strength data. Concrete strength data shall be based on tests of field-cured cylinders or, when approved by the building official, on other procedures to evaluate concrete strengths.

ACI 318 §6.2.2.2. No construction loads exceeding the combination of superimposed dead load plus specified live load shall be supported on any unshored portion of the structure under construction, unless analysis indicates adequate strength to support such additional loads.

ACI 318 §6.2.2.3. Form supports for prestressed concrete members shall not be removed until sufficient prestressing has been applied to enable prestressed members to carry their dead load and anticipated construction loads.

The ACI 318 Commentary explains that in determining the time for removal of forms, consideration should be given to the construction loads and to the possibility of deflections. The construction loads are frequently at least as great as the specified live loads. At early ages, a structure may be adequate to support the applied loads but may deflect sufficiently to cause permanent damage. It is further stated in the commentary that:

The removal of formwork for multistory construction should be a part of a planned procedure considering the temporary support of the whole structure as well as that of each individual member. Such a procedure should be worked out prior to construction and should be based on a structural analysis taking into account the following items, as a minimum:

(a) the structural system that exists at the various stages of construction and the construction loads corresponding to those stages;

(b) the strength of the concrete at the various ages during construction;

(c) the influence of deformations of the structure and shoring system on the distribution of dead loads and construction loads during the various stages of construction;

(d) the strength and spacing of shores or shoring systems used, as well as the method of shoring, bracing, shore removal, and reshoring including the minimum time intervals between the various operations; and

(e) Any other loading or condition that affects the safety or serviceability of the structure during construction.

For multistory construction, the strength of the concrete during the various stages of construction should be substantiated by field-cured test specimens or other approved methods.

It should be noted that the above requirements of ACI 318 and the accompanying suggestions in the commentary, while fairly comprehensive and meaningful, do not necessarily reflect current practice. It is also of interest to note here that prescriptive detailing requirements for structural integrity were added for the first time to the 1989 edition of the ACI 318 standard for cast-in-place concrete structures. Similar requirements were added to ACI 318-95 for precast concrete structures. The requirements were prompted by experience showing that the overall integrity of a structure can be substantially enhanced by minor changes in the detailing of reinforcement. It is the intent of Section 7.13 of ACI 318-95 (requirements for structural integrity) to improve the redundancy and ductility in structures so that, in the event of damage to a major supporting element or an abnormal loading event, the resulting damage may be confined to a relatively small area and the structure may have a better chance to maintain overall stability. Specifically for flat-plate and flat-slab construction, ACI 318-89 required that at least two of the column

strip bottom bars or wires in each direction should be made continuous, pass within the column core, and be anchored at exterior supports. Since its 1995 edition, ACI 318 has contained the following expanded requirements for flat plates or flat slabs:

ACI 318 §13.3.8.5. All bottom bars or wires within the column strip, in each direction, shall be continuous or spliced with Class A splices…At least two of the column strip bottom bars or wires in each direction shall pass within the column core and shall be anchored at exterior supports. The continuous column strip bottom reinforcement provides the slab with some residual ability to span to the adjacent supports, should a single support be damaged. A structural integrity provision has now also been added for other two-way slabs without beams:

ACI 318 §13.3.8.6. In slabs with shearheads and in lift-slab construction…, at least two bonded bottom bars or wires in each direction shall pass through the shearhead or lifting collar as close to the column as practicable and be continuous or spliced with a Class A splice. At exterior columns, the reinforcement shall be anchored at the shearhead or lifting collar.

References

ACI Committee 209. 1971. Prediction of creep, shrinkage and temperature effects in concrete structures. In *Designing for Creep, Shrinkage, and Temperature in Concrete Structures*, SP-27, pp. 51–93. American Concrete Institute, Farmington Hills, MI.

ACI Committee 318. 1995. *Building Code Requirements for Structural Concrete and Commentary.* ACI 318-95 and ACI 318R-95, 370 pp. American Concrete Institute, Farmington Hills, MI.

ACI Committee 318. 2005. *Building Code Requirements for Structural Concrete and Commentary.* ACI 318-05 and ACI 318R-05, 430 pp. American Concrete Institute, Farmington Hills, MI.

ACI Committee 347. 2004. *Guide to Formwork for Concrete*, ACI 347-04, 32 pp. American Concrete Institute, Farmington Hills, MI.

ACI Committee 435. 1995. *State-of-the-Art Report on Control of Two-Way Slab Deflections*, ACI 435-9R-95 (reapproved 2000), 14 pp. American Concrete Institute, Farmington Hills, MI.

Agarwal, R.K. and Gardner, N.J. 1974. Form and shore requirements for multistory flat slab type buildings. *ACI J. Proc.*, 71(11): 559–569.

ANSI. 1997. *American National Standard for Construction and Demolition Operation—Concrete and Masonry Work—Safety Requirements*, ANSI A10.9-1997, 22 pp. American National Standards Institute, Washington, D.C.

Beresford, F.D. 1964. An analytical examination of propped floors in multistory flat plate construction. *Construct. Rev.*, 37(11), 16–20.

Beresford, F.D. 1971. Shoring and reshoring of floors in multistory buildings. In *Symposium on Formwork*, pp. 559–569. Concrete Institute of Australia, North Sydney.

Blakey, F.A. and Beresford, F.D. 1965. Stripping of formwork for concrete in buildings in relation to structural design. *Civil Eng. Trans. Inst. Eng. Australia*, 7(2), 92–96.

Branson, D.E. 1977. *Deformation of Concrete Structures.* McGraw-Hill, New York.

Byfors, J. 1980. *Plain Concrete at Early Ages*, Fo. 3, No. 80, 566 pp. Swedish Cement and Concrete Research Institute, Stockholm, Sweden.

Cantor, I.G. and Rizzi, A.V. 1982. Shore and reshore procedures for flat slabs. In *Proceedings of the First International Conference on Forming Economical Concrete Buildings*, Lincolnshire, IL, November 8–10, pp. 18.1–18.12. Portland Cement Association, Skokie, IL.

Carino, N.J. and Lew, H.S. 1982. Re-examination of the relation between splitting tensile and compressive strength of normal weight concrete. *ACI J. Proc.*, 79(3), 214–219.

CEB. 1964. *Recommendations for an International Code of Practice for Reinforced Concrete*. Bulletin D'Information, No. 80, Comité Européen du Béton (CEB), Paris.

CEB. 1972. *Manual: Structural Effects of Time-Dependent Behavior of Concrete*. Bulletin D'Information, No. 80, Comité Européen du Béton (CEB), Paris.

City of Boston. 1971. *The Building Collapse of 2000 Commonwealth Avenue, Boston, Massachusetts*, Report, Mayor's Investigating Commission, 159 pp. Boston, MA.

Fattal, S.G. 1983. *Evaluation of Construction Loads in Multistory Concrete Buildings*. NBS Building Science Series No. 146, 130 pp. National Bureau of Standards, Washington, D.C.

Fintel, M. Iyengar, S.H., and Ghosh, S.K. 1987. *Column Shortening in Tall Structures: Prediction and Compensation*, EB108-01D. Portland Cement Association, Skokie, IL.

Fu, H.C. and Gardner, N.J. 1986. Effect of high early-age construction loads on the long term behavior of slab structures. In *Properties of Concrete at Early Ages*, SP-95, pp. 173–200. American Concrete Institute, Farmington Hills, MI.

Gardner, N.J. 1960. Relationship of the punching shear capacity of reinforced concrete slabs with concrete strength. *ACI J. Proc.*, 87(1), 66–71.

Gardner, N.J. 1985. Shoring, reshoring, and safety. *Concrete Int.*, 7(4), 28–34.

Gardner, N.J. and Poon, S.M. 1976. Time and temperature effects on tensile, bond and compressive strengths. *ACI J. Proc.*, 73(7), 405–409.

Grundy, P. and Kabaila, A. 1963. Construction loads on slabs with shored formwork in multistory buildings. *ACI J. Proc.*, 60(12), 1729–1738.

Hansen, T.C. and Mattock, A.H. 1966. Influence of size and shape of member on the shrinkage and creep of concrete. *ACI J. Proc.*, 63(2), 267-289.

Hickey, K.B. 1968. *Creep of Concrete Predicted from Elastic Modulus Tests*, Report No. C-1242. U.S. Department of the Interior, Bureau of Reclamation, Denver, CO.

Hover, K.C. 1984. The Effects of Moisture on the Physical Properties of Hardened Concrete and Mortar, Ph.D. thesis. Cornell University, Ithaca, NY.

Hover, K.C. 1988. The effects of drying and form and shore removal on flexural cracking in beams and slabs. In *Forming Economical Concrete Buildings: Proceedings of the Third International Conference*, SP107, pp. 169–184. American Concrete Institute, Farmington Hills, MI.

Hurd, M.K. 2005. *Formwork for Concrete*, 7th ed., SP-4, 500 pp. American Concrete Institute, Farmington Hills, MI.

Kaminetzky, D. and Stivaros, P.C. 1994. Early-age concrete: construction loads, behavior and failures. *Concrete Int.*, 16(1), 58–63.

Klieger, P. 1958. Effect of mixing and curing temperature on concrete strength. *ACI J. Proc.*, 29(12), 1063–1081.

Lasisi, M.Y. and Ng, S.F. 1979. Construction loads imposed on high-rise floor slabs. *Concrete Int.*, 1(2), 24–29.

Lew, H.S. 1985. Construction loads and load effects in concrete building construction. *Concrete Int.*, 7(4), 20–23.

Lew, H.S. and Reichard, T.W. 1978. Mechanical properties of concrete at early ages. *ACI J. Proc.*, 75(10), 533–542.

Lew, H.S., Carino, N.J., Fattal, S.G., and Batts, M.E. 1982a. *Investigation of the Construction Failure of Harbour Cay Condominium in Cocoa Beach, FL*. NBS Building Science Series No. 145. National Bureau of Standards, Washington, D.C.

Lew, H.S., Carino, N.J., and Fattal, S.G. 1982b. Cause of the condominium collapse in Cocoa Beach, FL. *Concrete Int.*, 4(8), 64–73.

Leyendecker, E.V. and Fattal, S.G. 1977. *Investigation of the Skyline Plaza Collapse in Fairfax County, Virginia*, Building Science Series No. 94, 88 pp. National Bureau of Standards, Washington, D.C.

Liu, X.-L., Chen, W.-F., and Bowman, M.D. 1985a. Construction loads on supporting floors. *Concrete Int.*, 7(12), 21–26.

Liu, X., Chen, W.-F., and Bowman, M.D. 1985b. Construction load analysis for concrete structures. *J. Struct. Eng. ASCE*, 111(5), 1019–1036.

Marosszeky, M. 1972. Construction loads in multistory structures. *Civil Eng. Trans. Inst. Eng. Australia*, 14(1), 91–93.

Nawy, E.G. 2008. *Reinforced Concrete: A Fundamental Approach*, 6th ed., 934 pp. Prentice Hall, Upper Saddle River, NJ.

Neville, A.M. 1995. *Properties of Concrete*, 4th ed., 844 pp. Longman, London.

Nielsen, K.E.C. 1952. *Loads on Reinforced Concrete Floor Slabs and Their Deformations during Construction*. Proc. No. 15, 113 pp. Swedish Cement and Concrete Research Institute, Stockholm.

Pauw, A. 1960. Static modulus of elasticity of concrete as affected by density. *ACI J. Proc.*, 57(6), 679–687.

Pfeifer, D.W., Magura, D.D., Russell, H.G., and Corley, W.G. 1971. Time-dependent deformations in a 70-story structure. In *Designing for Creep, Shrinkage, and Temperature in Concrete Structures*, SP-27, pp. 159–185. American Concrete Institute, Farmington Hills, MI.

Price, W.H. 1951. Factors influencing concrete strength. *ACI J. Proc.*, 22(6), 417–432.

RILEM Commission 42-CEA. 1981. Properties of set concrete at early ages: state-of-the-art report. *Mater. Struct.*, 14(84), 399–450.

Russell, H.G. and Corley, W.G. 1977. *Time-Dependent Behavior of Columns in Water Tower Place*, RD025B, 10 pp. Portland Cement Association, Skokie, IL.

Sbarounis, J.A. 1984. Multistory flat plate buildings: construction loads and immediate deflections. *Concrete Int.*, 6(2), 70–77.

Scanlon, A. 1987. Excessive slab deflection: a serviceability failure. *J. Forensic Eng.*, 1(2), 21–29.

Stivaros, P.C. and Halvorsen, G.T. 1990. Shoring/reshoring operations for multistory buildings. *ACI Struct. J.*, 87(5), 589–596.

Stivaros, P.C. and Halvorsen, G.T. 1991. Equivalent frame analysis of concrete buildings during construction. *Concrete Int.*, 13(8), 57–62.

Stivaros, P.C. and Halvorsen, G.T. 1992. Construction load analysis of slabs and shores using microcomputers. *Concrete Int.*, 14(8), 27–32.

Taylor, P.J. 1967. Effects of formwork stripping time on deflections of flat slabs and plates. *Australian Civil Eng. Const.*, 8(2), 31–35.

Taylor, P.J. and Heiman, J.L. 1977. Long-term deflections of reinforced concrete flat slabs and plates. *ACI J. Proc.*, 74(11), 556–561.

Troxell, G. E. Davis, H.E., and Kelly, J.W. 1968. *Composition and Properties of Concrete*, 2nd ed. McGraw-Hill, New York.

Walker, S. and Bloem, D.L. 1957a. Effects of curing and moisture distribution on measured strength of concrete. *Highway Res. Rec.*, 36, 334–346.

Walker, S. and Bloem, D.L. 1957b. Studies of flexural strength of concrete. Part 3. Effects of variations in testing procedures. *Proc. Am. Soc. Test. Mater.*, 57, 1122–1142.

Wheen, R.J. 1982. An invention to control construction floor loads in tall concrete buildings. *Concrete Int.*, 4(5), 56–62.

Winter, G. and Nilson, A.H. 1991. *Design of Concrete Structures*, 11th ed. McGraw-Hill, New York.

(a)

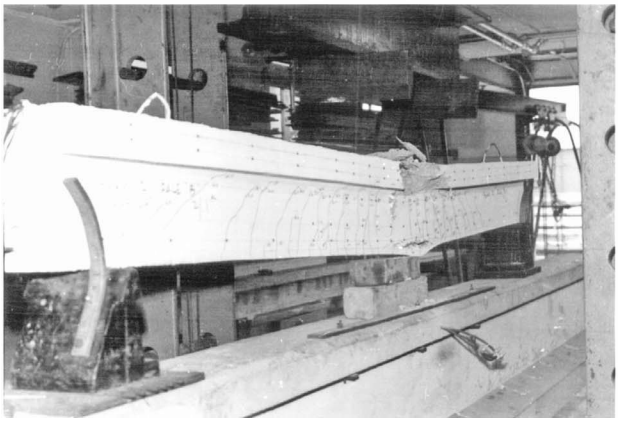

(b)

(a) Deflection test of a prestressed beam. (Photograph courtesy of Portland Cement Association, Skokie, IL.) (b) Deflection of a prestressed concrete beam prior to failure. (Photograph courtesy of Edward G. Nawy, Rutgers University.)